




# Inhibition of AIM2 inflammasome activation by a novel transcript isoform of IFI16

Pei-Hui Wang<sup>1</sup> , Zi-Wei Ye<sup>2</sup>, Jian-Jun Deng<sup>1</sup>, Kam-Leung Siu<sup>1</sup>, Wei-Wei Gao<sup>1</sup>, Vidyant Chaudhary<sup>1</sup> , Yun Cheng<sup>1</sup>, Sin-Yee Fung<sup>1</sup>, Kit-San Yuen<sup>1</sup>, Ting-Hin Ho<sup>1</sup>, Ching-Ping Chan<sup>1</sup>, Yan Zhang<sup>3</sup>, Kin-Hang Kok<sup>2</sup>, Wanling Yang<sup>3</sup>, Chi-Ping Chan<sup>1</sup> & Dong-Yan Jin<sup>1,\*</sup> 

## Abstract

Mouse p202 is a disease locus for lupus and a dominant-negative inhibitor of AIM2 inflammasome activation. A human homolog of p202 has not been identified so far. Here, we report a novel transcript isoform of human IFI16-designated IFI16- $\beta$ , which has a domain architecture similar to that of mouse p202. Like p202, IFI16- $\beta$  contains two HIN domains, but lacks the pyrin domain. IFI16- $\beta$  is ubiquitously expressed in various human tissues and cells. Its mRNA levels are also elevated in leukocytes of patients with lupus, virus-infected cells, and cells treated with interferon- $\beta$  or phorbol ester. IFI16- $\beta$  co-localizes with AIM2 in the cytoplasm, whereas IFI16- $\alpha$  is predominantly found in the nucleus. IFI16- $\beta$  interacts with AIM2 to impede the formation of a functional AIM2-ASC complex. In addition, IFI16- $\beta$  sequesters cytoplasmic dsDNA and renders it unavailable for AIM2 sensing. Enforced expression of IFI16- $\beta$  inhibits the activation of AIM2 inflammasome, whereas knockdown of IFI16- $\beta$  augments interleukin-1 $\beta$  secretion triggered by dsDNA but not dsRNA. Thus, cytoplasm-localized IFI16- $\beta$  is functionally equivalent to mouse p202 that exerts an inhibitory effect on AIM2 inflammasome.

**Keywords** AIM2; IFI16; inflammasome; transcript isoform

**Subject Categories** Immunology; Microbiology, Virology & Host Pathogen Interaction; Signal Transduction

**DOI** 10.15252/embr.201845737 | Received 4 January 2018 | Revised 13 July 2018 | Accepted 23 July 2018 | Published online 13 August 2018

**EMBO Reports (2018) 19: e45737**

## Introduction

Cyclic GMP-AMP synthase (cGAS) and AIM2 are master cytoplasmic double-stranded DNA (dsDNA) sensors [1]. Upon activation by dsDNA, cGAS produces a cyclic dinucleotide second messenger 2'3'-cGAMP, which binds with and activates endoplasmic reticulum membrane protein STING. Activated STING recruits TBK1 kinase to phosphorylate transcription factor IRF3, resulting in the production

of type I interferons (IFNs) [2]. On the other hand, cytoplasmic dsDNA sensing by AIM2 induces the activation of inflammasome, which is a cytoplasmic multi-protein complex that not only provides host defense against microbial pathogens but also contributes to pathogenic inflammation [3]. One recent study also suggested that dsDNA could induce inflammasome activation through an AIM2-independent cGAS-STING-NLRP3 pathway in human myeloid cells [4].

AIM2 contains an N-terminal effector pyrin domain (PYD) and a C-terminal HIN domain [5,6]. Whereas the positively charged HIN domain embraces dsDNA, PYD facilitates the recruitment of the inflammasome adapter protein ASC [7]. AIM2 resides in the cytoplasm and binds dsDNA from DNA viruses and bacteria [8–10]. Upon DNA binding, AIM2 recruits ASC via homotypic interaction of PYDs. ASC in turn recruits procaspase 1 through CARD–CARD interaction, resulting in the cleavage of prointerleukin-1 $\beta$  (pro-IL-1 $\beta$ ) and pro-IL-18, leading to the secretion of mature IL-1 $\beta$  and IL-18 [3]. AIM2 inflammasome is also activated in response to various types of cellular stress such as irradiation, nuclear membrane breakdown, and DNA damage [11]. Particularly, pharmacological disruption of nuclear envelope integrity by nelfinavir, which is commonly used in antiretroviral therapy as an inhibitor of viral proteases, can also activate AIM2 inflammasome by triggering the leakage of nuclear DNA to the cytoplasm [12].

AIM2 is one of the pyrin and HIN domain-containing (PYHIN) proteins which typically possess an N-terminal PYD and one or two C-terminal HIN domains [13,14]. There are only four human PYHIN proteins, namely AIM2, IFI16, IFIX, and MNDA, while at least 13 exist in mice, including Aim2/p210, p204, p202(a/b), p203, p205, p206, and MNDA-like. With the exception of AIM2 and possibly MNDA, the phylogenetic orthology among mammalian PYHIN proteins is not evident [13,14]. In contrast to AIM2, IFI16 predominantly localizes to the nucleus. IFI16 contains an N-terminal PYD and two C-terminal HIN domains, HIN A and HIN B, which cooperate to bind dsDNA [15,16]. IFI16 senses replicating DNA of herpesviruses in the nucleus and assembles an ASC- and procaspase-1-containing inflammasome, resulting in the formation of IFI16-ASC-caspase-1 inflammasome complex and AIM2-independent

<sup>1</sup> School of Biomedical Sciences, The University of Hong Kong, Pokfulam, Hong Kong

<sup>2</sup> Department of Microbiology, The University of Hong Kong, Pokfulam, Hong Kong

<sup>3</sup> Department of Pediatrics and Adolescent Medicine, The University of Hong Kong, Pokfulam, Hong Kong

\*Corresponding author. Tel: +852 3917 9491; Fax: +852 2855 1254; E-mail: dyjin@hku.hk

processing of pro-IL-1 $\beta$  [17–19]. Cytoplasmic localization of IFI16 in macrophages and lymphocytes might allow it to sense DNA, promote cGAMP production, and induce STING-dependent type I IFN expression [20]. IFI16 could also act as a host DNA sensor of HIV proviral DNA to trigger pyroptosis of abortively infected CD4 T cells [21,22]. The dynamic shuttling of IFI16 between the cytoplasm and nucleus is controlled by acetylation of the nuclear localization signal (NLS), allowing IFI16 to function as a nuclear and cytoplasmic DNA sensor [16,23]. Mouse p204, which has a similar domain organization as IFI16, also acts as a cytoplasmic DNA sensor to induce STING-dependent type I IFN expression [15]. In contrast, mouse p205 induces the expression of ASC mRNA to mediate inflammasome activation [24]. IFI16 serves as a DNA sensor to induce type I IFN production [15]. IFI16 also cooperates with cGAS in DNA sensing [20,25,26]. However, IFN response to cytoplasmic DNA was unaffected in mice deficient of all 13 AIM2-like PYHIN proteins, providing *in vivo* evidence that p204 is dispensable for DNA sensing coupled to type I IFN production [27]. Further investigations are required to resolve these discrepancies.

Mouse p202, with two tandem HIN domains homologous to those of IFI16 but lacking a PYD, can act as a negative regulator of AIM2 inflammasome through protein–protein interaction and dsDNA sequestration [28–30]. The HIN A domain of p202 has a higher affinity to dsDNA and its HIN B domain binds AIM2 HIN domain, separating it from PYDs to prevent ASC recruitment and clustering [29,30]. Several lines of evidence suggested p202 to be a susceptibility gene to systemic lupus erythematosus (SLE) in mice [31,32]. SLE is an autoimmune disease characterized by chronic stimulation of the innate immune system by endogenous nucleic acids, resulting in increased levels of type I IFNs [33]. p202 expression is elevated in SLE-susceptible mouse strains such as NZB and B6.Nba2 [28,31,32]. In line with this, the activity of AIM2 inflammasome is very low in macrophages of NZB mice [28]. p202 might contribute to SLE development through regulation of AIM2 inflammasome [32,34,35]. p202 is also implicated in the progression of other autoimmune diseases such as glomerulonephritis [36]. Type I IFN receptor-deficient mice that do not develop lupus show decreased expression of p202 [37]. Up to date, no human homolog of p202 or any human PYHIN protein with HIN domains only has been identified [13,14].

In this study, we identified and characterized a previously unrecognized transcript isoform of IFI16-designated IFI16- $\beta$ . Our results revealed the structural and functional similarity between IFI16- $\beta$  and mouse p202. IFI16- $\beta$  might serve to put a brake on excessive activation of AIM2 inflammasome.

## Results

### Identification and expression analysis of IFI16- $\beta$

Mouse p202 containing HIN A and HIN B domains only is a critical negative regulator of AIM2 inflammasome activation [28–30]. None of the four human PYHIN proteins AIM2, IFI16, IFIX, and MNDA has a similar structure, but IFI16 is the only one harboring both HIN A and HIN B domains. Given that multiple transcript and splicing isoforms are commonly found for human genes [38], we wondered whether there exist any IFI16 isoforms that contain the HIN domains only but lack any PYD. A search of the expressed sequence tag (EST)

database led to the identification of multiple ESTs with a putative transcription initiation site within intron 2 of IFI16. Further analysis revealed that all ESTs in this group derived from one alternative IFI16 transcript that encodes a protein with HIN A and HIN B domains but without PYD (GenBank accession number MH445452). Rapid amplification of cDNA ends yielded the same 5' sequence as one EST initiating from intron 2 of IFI16. To distinguish the two IFI16 transcripts, the newly identified transcript with an alternative 5' exon transcribed from intron 2 was named IFI16- $\beta$  and the original transcript became IFI16- $\alpha$  hereafter. The three previously identified splice isoforms of IFI16- $\alpha$  were known as A, B, and C, which have the same transcription start site and an identical 5' exon organization (Fig 1A) [39]. IFI16- $\beta$  is 162 amino acids shorter than the major and commonest isoform IFI16- $\alpha$ -B, which was also used for comparison throughout our study. Consistent with the presence of an alternative promoter, a DNase I hypersensitivity cluster as well as regions enriched with H3K4me1 and H3K27ac histone marks was found immediately upstream of the putative transcription initiation site of IFI16- $\beta$  in the ENCODE database. In addition, binding sites for multiple transcription factors such as STAT1, JUN, and FOS, some of which were also found in the promoter of other IFN-stimulated genes [40], were identified in the same upstream region.

We next sought to determine the expression patterns of endogenous IFI16- $\alpha$  and IFI16- $\beta$  in different human tissues and cells. Two pairs of isoform-specific primers were designed so that a fragment of correct size can only be amplified from IFI16- $\beta$  cDNA, but not from IFI16- $\alpha$  cDNA or genomic DNA, by the IFI16- $\beta$  primers. Likewise, the IFI16- $\alpha$  primers were specific to IFI16- $\alpha$  cDNA (Fig 1A). IFI16- $\beta$  mRNA was found in multiple human tissues and cell lines. Particularly, IFI16- $\beta$  mRNA was relatively more abundant in placenta, spleen, peripheral blood leukocytes, THP-1 monocytic cells, U937 histiocytic cells, and HuT102 lymphocytic cells (Fig 1B and C).

Although IFI16- $\beta$  transcript is expressed from an alternative promoter and has a unique 5' untranslated region, IFI16- $\beta$  protein is translated from the coding exons shared by IFI16- $\alpha$  and IFI16- $\beta$ . Thus, IFI16- $\beta$  is a truncated version of IFI16- $\alpha$  lacking the PYD domain (Fig 1A). To distinguish the expression of endogenous IFI16- $\alpha$  and IFI16- $\beta$  proteins, two monoclonal anti-IFI16 antibodies were purchased. The anti-IFI16N antibody (sc-8023 from Santa Cruz) was raised against the N-terminal PYD, while the other anti-IFI16C antibody (ab50004 from Abcam) recognized the shared C-terminal HIN B domain. In fact, when individual proteins were ectopically expressed in HEK293T cells, anti-IFI16N was only found reactive to IFI16- $\alpha$  but not IFI16- $\beta$ . In contrast, anti-IFI16C bound to both IFI16- $\alpha$  and IFI16- $\beta$  (Fig 1D). Moreover, multiple anti-IFI16C-reactive protein bands were seen in THP-1 cell lysate and they might correspond to the three known splice isoforms of IFI16- $\alpha$  (i.e., IFI16- $\alpha$ -A, IFI16- $\alpha$ -B, and IFI16- $\alpha$ -C). In addition to these three IFI16- $\alpha$  isoforms, an additional anti-IFI16C-reactive protein species compatible with the predicted size of IFI16- $\beta$  was also observed (Fig 1E and F). Upon treatment with IFN- $\beta$ , all IFI16- $\alpha$  and IFI16- $\beta$  bands became more prominent (Fig 1E). When cells were transfected with IFI16- $\beta$  isoform-specific siRNA, the fast-migrating anti-IFI16C-reactive band disappeared almost completely, lending crucial support to our argument that this band derives from endogenous IFI16- $\beta$  (Fig 1F). Collectively, these data indicated that IFI16- $\beta$  protein is expressed THP-1 cells and its expression can be further induced by IFN- $\beta$ .

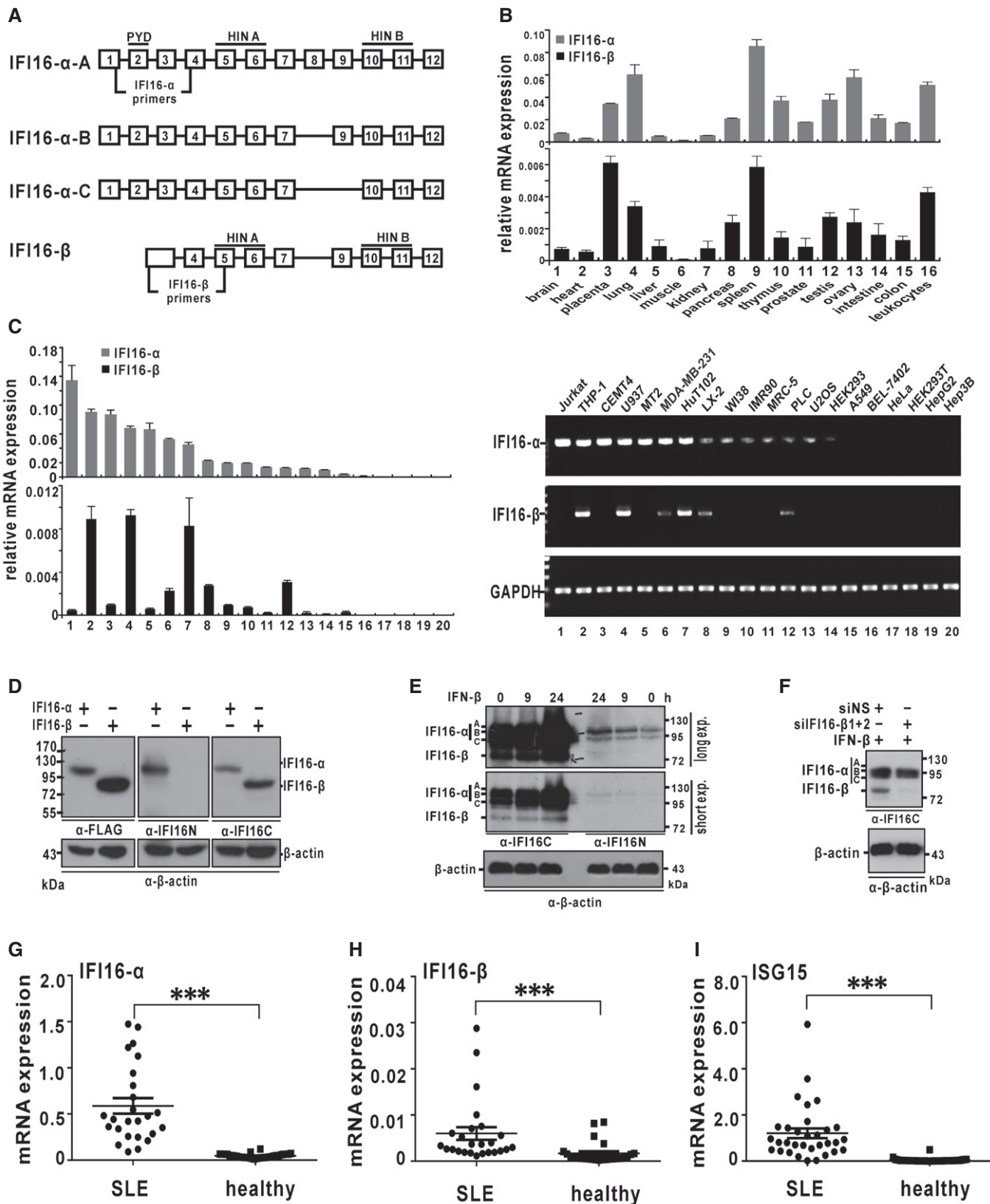


Figure 1.

**Figure 1. Expression analysis of IFI16- $\beta$ .**

- A Genome structure of IFI16- $\alpha$  and IFI16- $\beta$ . Boxes denote exons and lines represent introns. Positions of isoform-specific primers used in RT-PCR and RT-qPCR analysis are indicated. PYD, HIN A, and HIN B domains are also shown. Transcription of IFI16- $\beta$  mRNA is driven by an alternative promoter located within intron 2 of IFI16- $\alpha$ .
- B Distribution of IFI16- $\alpha$  and IFI16- $\beta$  in human tissues. Human MTC™ Panels I and II (Clontech) containing cDNA templates of various human tissues were used for RT-qPCR analysis using isoform-specific primers. Relative mRNA expression was derived from  $2^{-\Delta\Delta Ct}$  by normalizing to the levels of glyceraldehyde-3-phosphate dehydrogenase (GAPDH) transcript. Three independent biological replicates were analyzed, and error bars indicate SD.
- C Distribution of IFI16- $\alpha$  and IFI16- $\beta$  in human cell lines by isoform-specific RT-qPCR (left) and RT-PCR (right). Three independent biological replicates were analyzed and error bars indicate SD.
- D Immunoblot analysis of recombinant IFI16- $\alpha$  and IFI16- $\beta$  expressed in HEK293T cells using anti-FLAG ( $\alpha$ -FLAG), anti-IFI16 N-terminal ( $\alpha$ -IFI16N), and anti-IFI16 C-terminal ( $\alpha$ -IFI16C) antibodies.
- E Induced expression of endogenous IFI16- $\alpha$  and IFI16- $\beta$  in THP-1 cells treated with recombinant IFN- $\beta$  (1000 U/ml). Both long and short exposures (exp.) of the same IFI16 blot are shown.
- F Specific knockdown of the expression of endogenous IFI16- $\beta$  in THP-1 cells by a combination of two siRNAs targeting IFI16- $\beta$  (siIFI16- $\beta$ 1+2). siNS in the non-specific control group is an irrelevant siRNA.
- G-I mRNA expression levels of IFI16- $\alpha$ , IFI16- $\beta$ , and IFN-stimulated gene ISG15 in SLE patients and healthy individuals. Total RNA of PBMCs from SLE patients and healthy individuals ( $n = 24$ ) was isolated and reverse-transcribed into first-strand cDNA. The expression of IFI16- $\alpha$ , IFI16- $\beta$ , and ISG15 mRNAs was determined by RT-qPCR. Results were presented as dot plots showing the spread of data with the medians as well as upper and lower quartiles indicated by the three horizontal bars. Student's *t*-test was performed to assess statistical significance of the differences between SLE patients and healthy subjects, with *P* values lower than 0.001 highlighted by \*\*\*.

Data information: Three independent immunoblotting experiments were carried out with similar results. Source data are available online for this figure.

SLE is an interferonopathy in which type I IFNs are highly induced and hyperactive [33,34]. To determine whether IFI16- $\beta$  might also be induced in SLE patients, RT-qPCR was performed with peripheral blood mononuclear cells (PBMCs) isolated from SLE patients and healthy subjects. Not to our surprise, both IFI16- $\alpha$  and IFI16- $\beta$  were significantly upregulated in PBMCs of SLE patients (Fig 1G and H). The induction pattern was also similar to that of ISG15, a well-known IFN-stimulated gene (Fig 1I). Thus, both IFI16- $\alpha$  and IFI16- $\beta$  were likely induced by type I IFNs. As a result, their expression was aberrantly upregulated in SLE.

**IFN- $\beta$  inducibility of IFI16- $\beta$** 

Above we have shown the responsiveness of IFI16- $\beta$  protein expression to IFN- $\beta$  (Fig 1E) and the upregulation of IFI16- $\beta$  in SLE (Fig 1H). Multiple binding sites for STAT1 and other transcription factors were also found in the putative IFI16- $\beta$  promoter. The functionality of the STAT1 sites has already been demonstrated in a previous ChIP-seq study [41]. To verify promoter activity, we cloned IFI16- $\alpha$  and IFI16- $\beta$  promoter regions into pGL3 luciferase reporter. Fig 2A indicates that the basal activity of IFI16- $\alpha$  promoter was more pronounced than that of IFI16- $\beta$  promoter. However, the activity of both IFI16- $\alpha$  and IFI16- $\beta$  promoters was boosted remarkably when HEK293T cells were infected by herpes simplex virus (HSV)-1- $\Delta$ ICP0, vesicular stomatitis virus (VSV)-GFP, or Sendai virus (SeV). Because one major virus-encoded IFN antagonist had been deleted from HSV-1- $\Delta$ ICP0, its ability to induce IFN- $\beta$  was considerably higher than that of the wild-type HSV-1 [42]. Similar stimulatory effect was also observed when cells were treated with IFN- $\beta$  or poly (I:C) or transfected with MAVS, an essential mitochondrial stimulator of IFN production (Fig 2A). Although the basal activity of IFI16- $\beta$  promoter was less pronounced, its inducibility by IFN- $\beta$  and other stimuli in terms of fold change was not less prominent than that of IFI16- $\alpha$ . Thus, IFI16- $\beta$  promoter was functional, responsive to IFN- $\beta$  and independent of IFI16- $\alpha$  promoter.

Consistent with the above results, the expression of both IFI16- $\alpha$  and IFI16- $\beta$  transcripts in THP-1 cells was potently induced by

IFN- $\beta$  over a time course. However, the induction patterns of IFI16- $\alpha$  and AIM2 transcripts were similar but distinct from that of IFI16- $\beta$  (Fig 2B). Likewise, IFI16- $\alpha$ , IFI16- $\beta$ , and AIM2 transcripts were also inducible by dsDNA90mer and HSV-1- $\Delta$ ICP0 (Fig 2C and D). Finally, to explore whether protein kinase C might regulate IFI16- $\alpha$  and IFI16- $\beta$  expression, we treated the cells with its activator 12-O-tetradecanoylphorbol-13-acetate (TPA). Whereas IFI16- $\alpha$  and AIM2 mRNAs were induced by TPA most robustly at 24 and 36 h after treatment, the induction of IFI16- $\beta$  by TPA occurred earlier at 3 h and plateaued at 9 h (Fig 2E). Collectively, these results corroborated the IFN- $\beta$  inducibility of IFI16- $\beta$  promoter and suggested that it is regulated independently of IFI16- $\alpha$  promoter.

**Subcellular localization of IFI16- $\beta$** 

Subcellular localization of IFI16- $\alpha$  might be critical to its function as a nuclear and cytoplasmic DNA sensor [16,43]. The cytoplasmic localization of IFI16- $\beta$  is predicted by its lack of NLS1 and NLS2. Indeed, whereas IFI16- $\alpha$  was confined to the nucleus in resting HeLa cells, IFI16- $\beta$  was predominantly found in the cytoplasm (Fig 3A, panels 4–6 compared to 1–3). This was similar to the cytoplasmic localization pattern of IFI16- $\alpha$  $\Delta$ NLS1, in which NLS1 had been deleted (Fig 3A, panels 7–9). Thus, distinct from IFI16- $\alpha$ , IFI16- $\beta$  was a cytoplasmic protein. As such, IFI16- $\beta$  co-localized substantially with either ectopically expressed AIM2 in HeLa cells (Fig 3B, panels 6–8) or endogenous AIM2 in differentiated THP-1 cells (Fig 3C, panels 2–4). In contrast, IFI16- $\alpha$  and AIM2 were exclusively present in the cytoplasm and the nucleus, respectively (Fig 3B, panels 2–4). These results indicated the cytoplasmic localization of IFI16- $\beta$  and its co-localization with AIM2.

**IFI16- $\beta$  associates with STING and weakly induces IFN- $\beta$  production**

The cytoplasmic fraction of IFI16 is thought to induce type I IFN production through STING in cooperation with cGAS [20,26]. The cytoplasmic localization of IFI16- $\beta$  prompted us to investigate its



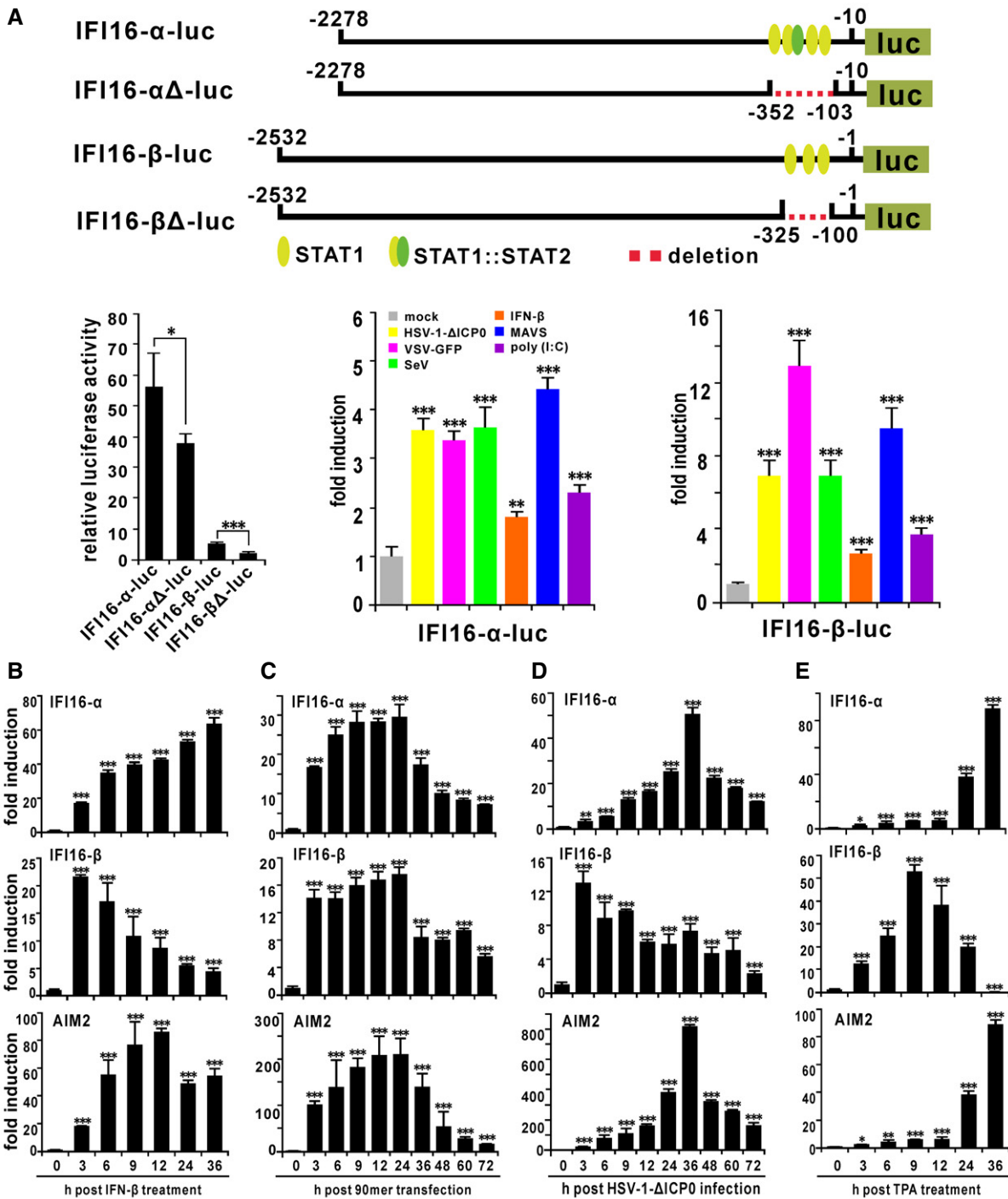


**Figure 2. Induction patterns of IFI16- $\alpha$  and IFI16- $\beta$ .**

**A** Promoter analysis and induction patterns. IFI16- $\alpha$  (nucleotides -2278 to -10, with translation start site set as 1) and IFI16- $\beta$  (nucleotides -2532 to -1) promoters were individually cloned into pGL3 luciferase reporter construct to generate IFN16- $\alpha$ -luc and IFI16- $\beta$ -luc. Their promoter activities in HEK293T cells were measured by dual-luciferase assay. Cells were infected with HSV-1- $\Delta$ ICP0 (MOI = 5), VSV-GFP (MOI = 0.01), or SeV (80 HA/ml), treated with IFN- $\beta$  (1,000 U/ml), or transfected with MAVS plasmid or poly (I:C) (1.0  $\mu$ g/ml). The activity recovered from the mock-treated group transfected with pGL3 empty vector alone was set as 1. The differences between the indicated group and the mock were statistically significant as judged by Student's *t*-test (\**P* < 0.05, \*\**P* < 0.01 and \*\*\**P* < 0.001).

**B–E** Temporal expression profiles of IFI16- $\alpha$ , IFI16- $\beta$ , and AIM2 in THP-1 cells treated with recombinant IFN- $\beta$  (1,000 U/ml), transfected with dsDNA90mer (1.0  $\mu$ g/ml), infected with HSV-1- $\Delta$ ICP0 (MOI = 5), or treated with TPA (200 nM). Cells were harvested at the indicated time points for total RNA extraction. IFI16- $\alpha$ , IFI16- $\beta$ , and AIM2 transcripts were determined by RT-qPCR. The differences between the indicated group and the control at time zero were statistically significant as judged by Student's *t*-test (\**P* < 0.05, \*\**P* < 0.01 and \*\*\**P* < 0.001).

Data information: All bars represent the means  $\pm$  SD (*n* = 3).

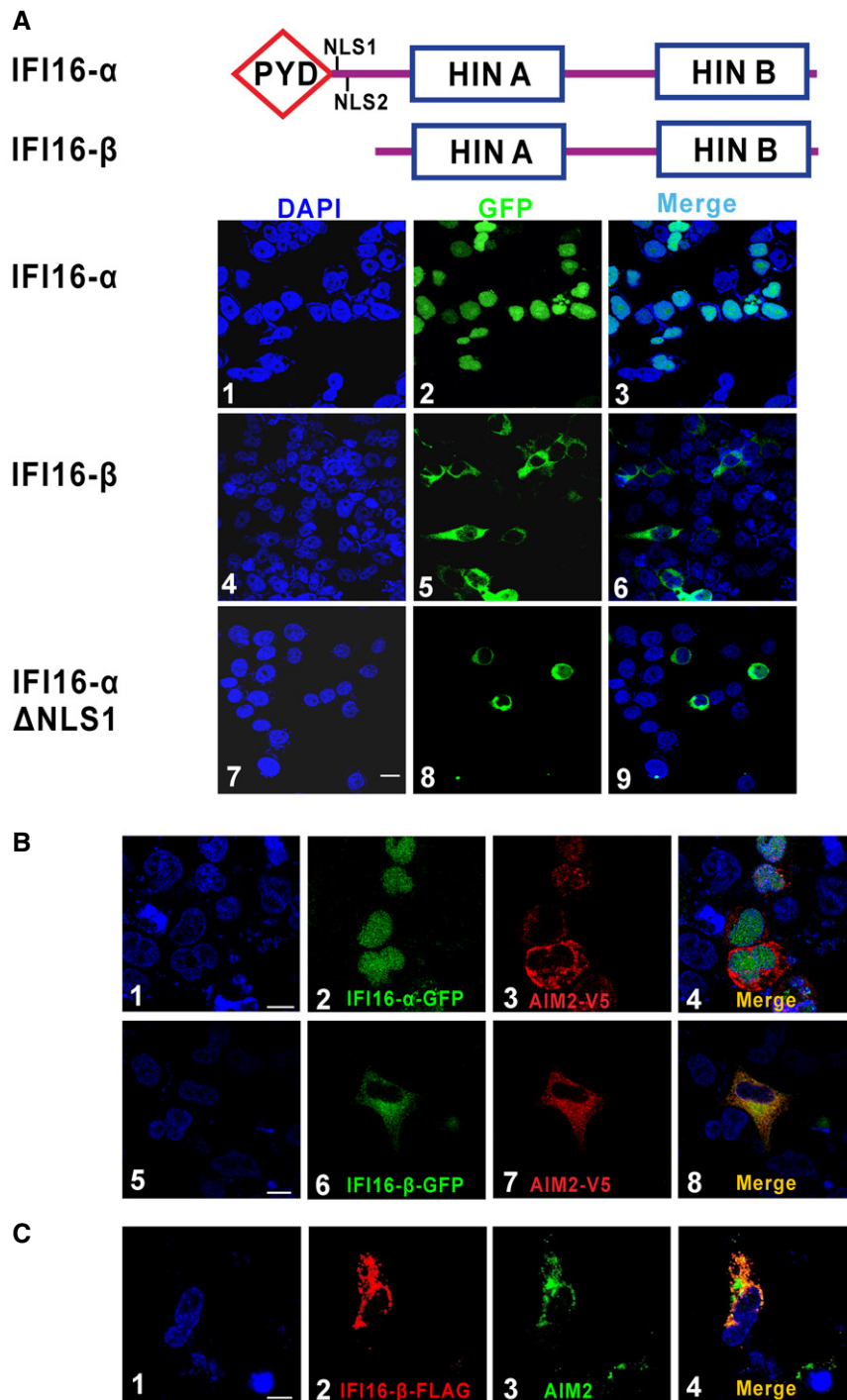


**Figure 3. Subcellular localization of IFI16- $\alpha/\beta$  and their co-localization with AIM2.**

**A** Subcellular localization. HeLa cells were transfected individually with plasmids pcDNA6-IFI16- $\alpha$ -eGFP, pcDNA6-IFI16- $\beta$ -eGFP, and pcDNA6-IFI16- $\alpha$  $\Delta$ NLS1-eGFP. After 36 h, cells were fixed, stained, and subjected to confocal microscopy. Nuclei were visualized with DAPI (blue). Scale bar, 20  $\mu$ m.

**B** Co-localization of IFI16- $\beta$  but not IFI16- $\alpha$ , with AIM2 in the cytoplasm. Plasmid pcDNA6-IFI16- $\alpha$ -GFP or pcDNA6-IFI16- $\beta$ -GFP was co-transfected into HeLa cells together with pcDNA3.1-AIM2-V5. After 36 h, cells were fixed with 4% paraformaldehyde. After blocking, cells were incubated with mouse anti-V5 and then goat anti-mouse IgG conjugated to tetramethylrhodamine (red) to stain for AIM2. Co-localization in the merged image is in yellow. Scale bars, 20  $\mu$ m.

**C** Co-localization of IFI16- $\beta$  with endogenous AIM2 in THP-1-derived macrophages. THP-1 cells were transfected with IFI16- $\beta$ -FLAG plasmid. After 24 h, cells were treated with 200 nM of TPA for another 24 h to induce differentiation into macrophages. Cells were cultured for an additional 24 h in the absence of TPA and then fixed with 4% paraformaldehyde. After blocking, cells were incubated with mouse anti-FLAG (M2) and rabbit anti-AIM2 antibodies overnight at 4°C. After washing, the cells were incubated with tetramethylrhodamine-labeled goat anti-mouse IgG (red) to stain for IFI16- $\beta$  and with fluorescein-labeled goat anti-rabbit IgG (green) to stain for endogenous AIM2. Scale bar, 20  $\mu$ m.

Data information: Two independent experiments were performed with similar results.

impact on IFN- $\beta$  induction. In our setting, both IFI16- $\alpha$  and IFI16- $\beta$  were found to activate luciferase reporter gene expression driven by IFN- $\beta$  promoter (IFN- $\beta$ -luc), IRF3-binding elements (IRF3-luc), and IFN-stimulated response elements (ISRE-luc) only in HEK293 cells overexpressing either STING alone or STING plus cGAS (Fig 4A), indicating the requirement of STING and cGAS for their optimal induction of IFN- $\beta$ . Notably, the IFN- $\beta$ -inducing activity of IFI16- $\beta$  was less pronounced than that of IFI16- $\alpha$ . In line of this, specific knockdown of IFI16- $\beta$  by siRNAs exhibited a mild suppressive effect on dsDNA90mer-induced activation of IFN- $\beta$  and ISG54 mRNA expression in both THP-1 cells (Fig 4B) and human primary monocyte-derived macrophages (MDMs) derived from three different donors (Fig 4C and Appendix Fig S1). Generally consistent with the previous finding that the PYD-deleted mutant of IFI16- $\alpha$  was less competent in its cooperation with cGAMP or STING in the activation of IFN- $\beta$  production [20], our results suggested IFI16- $\beta$  to be a weak IFN- $\beta$  inducer.

Because the weak IFN- $\beta$ -inducing activity of IFI16- $\beta$  in HEK293 cells was only observed in the presence of STING (Fig 4A), we asked whether IFI16- $\beta$  might also interact with STING. Co-immunoprecipitation was performed, and IFI16- $\beta$  was found in the precipitates that contain human or mouse STING (Fig 4D). Similar STING-binding ability was also seen with IFI16- $\alpha$  and two other mouse PYHIN proteins p204 and p202. However, the PYD domain of IFI16- $\alpha$  was not sufficient for the binding with STING (Fig 4D, right panel). Consistent with the binding between IFI16- $\beta$  and STING, IFI16- $\beta$  co-localized with STING in HeLa cells and the co-localization was even more pronounced when cGAS was also overexpressed (Fig 4E). Notably, the discrete punctate staining pattern of STING in the cytoplasm of these cells was compatible with the notion that aggregate formation was required for its activation [44–46]. Thus, IFI16- $\beta$  interacts with and activates STING for type I IFN production.

#### IFI16- $\beta$ interacts with AIM2 to impede AIM2-ASC association

AIM2 inflammasome activation relies on the assembly of multi-protein complexes containing a sensor protein such as AIM2, the

adaptor protein ASC, and procaspase-1 [3]. Previous studies have shown that mouse p202 harnesses its HIN domains to physically interact with AIM2 and inhibit its activity [28–30]. To determine how IFI16- $\beta$  structurally related to p202 (Fig 5A) might affect AIM2 inflammasome activation, co-immunoprecipitation experiments were performed. Both IFI16- $\alpha$  and IFI16- $\beta$  were detected in the AIM2 immunoprecipitates (Fig 5B). We noted that AIM2-associated IFI16- $\beta$  was apparently more abundant than AIM2-associated IFI16- $\alpha$  (Fig 5B, lane 3 compared to 1), suggesting that AIM2 might preferentially form a complex with IFI16- $\beta$ . This was in agreement with the data showing co-localization of AIM2 and IFI16- $\beta$  (Fig 3B and C). The absence of AIM2 in the PYD-FLAG-containing immunoprecipitates further indicated that the interaction of AIM2 with IFI16- $\alpha$  was not mediated by PYD (Fig 5C). Given that the activation of AIM2 inflammasome requires the recruitment and clustering of ASC mediated by homotypic PYD interaction between AIM2 and ASC, we reasoned that the binding of IFI16- $\beta$  to AIM2 might create steric hindrance that impedes AIM2-ASC interaction. To test this model, competitive co-immunoprecipitation was carried out. Indeed, enforced expression of either IFI16- $\beta$  or p202 resulted in diminution of ASC being detected in the AIM2 immunoprecipitates (Fig 5D, lanes 3–6 compared to 2), suggesting that IFI16- $\beta$  might function in a manner similar to p202.

To extend our analysis to endogenous proteins in immune cells, reciprocal co-immunoprecipitation was carried out with cytosolic and nuclear fractions of THP-1-derived macrophages. Whereas IFI16- $\beta$  and AIM2 were primarily cytosolic, IFI16- $\alpha$  was concentrated in the nucleus. Immunoprecipitation with either mouse anti-IFI16C antibody recognizing endogenous IFI16- $\alpha$  and IFI16- $\beta$  or mouse anti-AIM2 antibody reacting with endogenous AIM2 revealed that AIM2 and IFI16- $\beta$  in the cytosolic fraction form a complex (Fig 5E, middle and right panels). Similar observation was also made in HeLa cells overexpressing IFI16- $\beta$  and then treated with IFN- $\beta$  to induce the expression of AIM2 (Fig 5F). Notably, although IFI16- $\alpha$  interacted with AIM2 in overexpression experiments performed in HEK293T (Fig 5B and C) and HeLa (Fig 5F) cells, they were in different subcellular fractions and therefore did not appear

#### Figure 4. Role of IFI16- $\beta$ in dsDNA-induced IFN- $\beta$ production.

- IFI16- $\beta$  is a weak activator of IFN- $\beta$  production in HEK293 cells. Cells were transfected with the indicated combinations of plasmids expressing IFI16- $\alpha$  (450 ng), IFI16- $\beta$  (450 ng), STING (20 ng) and cGAS (20 ng) together with IFN- $\beta$ -luc, IRF3-luc or ISRE-luc reporter (20 ng). pcDNA6 empty vector was used to equalize the total amount of transfected DNA. Dual-luciferase assays were performed 36 h after transfection. Three independent biological replicates were analyzed, and error bars indicate SD. The differences between the indicated groups were judged to be either statistically significant (\*\* $P < 0.01$  and \*\*\* $P < 0.001$ ) or not significant (NS) by Student's *t*-test.
- Knockdown of endogenous IFI16- $\beta$  in THP-1 cells impairs dsDNA-induced IFN- $\beta$  and ISG54 expression. Cells cultured in six-well plates were transfected with 1  $\mu$ l of either an irrelevant (siNS) or IFI16-targeting siRNA (100 nM) as indicated. After 48 h, THP-1 cells were transfected with dsDNA90mer (1,000 ng/ml) for 9 h and then collected for RT-qPCR analysis. Three independent biological replicates were analyzed and error bars indicate SD. The differences between the indicated group and the siNS control were statistically significant as judged by Student's *t*-test (\*\* $P < 0.01$  and \*\*\* $P < 0.001$ ).
- Knockdown of IFI16- $\beta$  in human MDMs diminishes dsDNA-induced IFN- $\beta$  and ISG54 expression. Human MDMs cultured in 24-well plates were repeatedly transfected with 0.5  $\mu$ l of the indicated siRNA (100 nM) for three times with a 24-h interval. After another 24 h, human MDMs were transfected with dsDNA90mer (1,000 ng/ml) twice with a 6-h interval. Human MDMs were then harvested and lysed. Three independent biological replicates were analyzed, and error bars indicate SD. The differences between the indicated group and the siNS control were statistically significant as judged by Student's *t*-test (\*\* $P < 0.01$  and \*\*\* $P < 0.001$ ).
- IFI16- $\beta$  interacts with STING. The indicated combinations of expression plasmids for human STING-HA (hSTING-HA or STING-HA; 1,000 ng), mouse STING-HA (mSTING-HA; 1,000 ng), IFI16- $\alpha$ -FLAG (9,000 ng), IFI16- $\beta$ -FLAG (9,000 ng), PYD-FLAG (9,000 ng), mouse p204-FLAG (9,000 ng), and mouse p202-FLAG (9,000 ng) were transfected into HEK293T cells. After 48 h, cells were harvested and lysed. Immunoprecipitation (IP) was carried out with mouse anti-HA or anti-FLAG antibody.
- Co-localization of IFI16- $\beta$  with STING. IFI16- $\beta$ -GFP and STING-HA plasmids were co-transfected with or without cGAS plasmid into HeLa cells. After 36 h, cells were fixed, blocked, and then incubated initially with mouse anti-HA for 12 h at 4°C and subsequently with goat anti-mouse IgG conjugated to tetramethylrhodamine (red) to stain for STING-HA. Nuclear morphology was revealed with DAPI (blue). Scale bars, 20  $\mu$ m.

Data information: Immunoblotting and confocal imaging results are representative of two independent experiments.

Source data are available online for this figure.

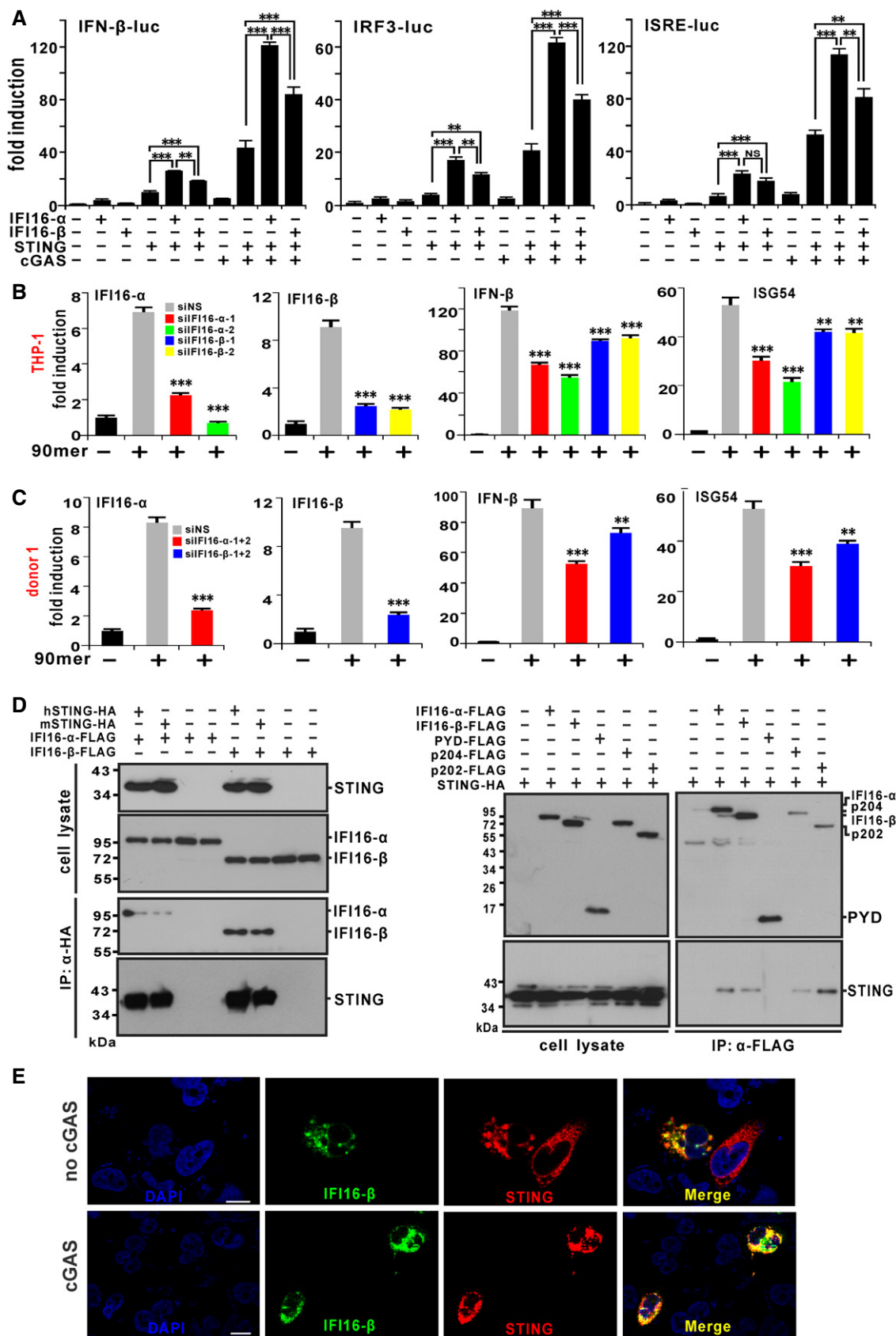


Figure 4.



in the same precipitate derived from differentiated THP-1 cells (Fig 5E). Furthermore, when we increased the expression of IFI16- $\alpha$  or IFI16- $\beta$  in differentiated THP-1 cells, the amount of ASC protein detected in the anti-AIM2 precipitate decreased progressively (Fig 5G, lanes 2 and 3 compared to 1 or lanes 5 and 6 compared to 4). Consistent with previous reports on p202 [28–30], these results suggested that IFI16- $\beta$  was capable of impeding AIM2-ASC interaction and AIM2 inflammasome complex assembly in a manner similar to p202.

### IFI16- $\beta$ binds with dsDNA to suppress AIM2-mediated dsDNA sensing

Both AIM2 and IFI16- $\alpha$  can directly bind with dsDNA [3]. IFI16- $\beta$  not only contains the complete HIN A and HIN B domains for dsDNA binding but also co-localizes with AIM2 in the cytoplasm (Fig 3B and C). With this in mind, we asked whether IFI16- $\beta$  might influence the binding of dsDNA to AIM2. Streptavidin beads were incubated with lysates of HEK293T cells transfected with biotinylated dsDNA90mer and different combinations of IFI16 plasmids to affinity-purify DNA–protein complex. Both IFI16- $\alpha$  and IFI16- $\beta$  were detected in a complex containing biotinylated dsDNA90mer (Fig 6A). This was consistent with the previous finding that HIN A and HIN B domains but not PYD can bind with dsDNA [7,47]. The IFI16- $\beta$  band detected in the dsDNA complex was more prominent, suggesting that it might bind tightly to dsDNA. Consistently, both AIM2 and IFI16- $\beta$  were pulled down by biotinylated dsDNA90mer (Fig 6B). Competition experiments indicated that non-biotinylated dsDNA90mer could effectively compete with biotinylated dsDNA90mer for binding with AIM2 and IFI16- $\beta$  (Fig 6B). Notably, more IFI16- $\beta$  than AIM2 was detected in the pull-down complex, suggesting that IFI16- $\beta$  might bind with a higher affinity to dsDNA than AIM2 (Fig 6B). These results are consistent with the previous finding that recombinant proteins containing the HIN A and HIN B domains only were capable of binding to dsDNA more robustly than AIM2 [7,15,29,30,47]. To determine whether

IFI16- $\beta$  could affect the binding of AIM2 to dsDNA, IFI16- $\beta$  and AIM2 were co-expressed in HEK293T cells. In agreement with results presented above, increasing expression of IFI16- $\beta$  correlated with diminished amounts of AIM2 detected in the DNA–protein complex containing biotinylated dsDNA90mer (Fig 6C, lanes 5 and 6 compared to 4), suggesting that IFI16- $\beta$  might compete with AIM2 for dsDNA binding. In keeping with this notion, when the expression of AIM2 was enhanced, less IFI16- $\beta$  was found in the dsDNA90mer-AIM2 complex (Fig 6C, lanes 11 and 12 compared to 10).

To verify our finding, protein–dsDNA co-immunoprecipitation was also carried out. In this experiment, fixed amount of AIM2 and increasing dose of IFI16- $\beta$  were expressed in HEK293T cells, which were further transfected with dsDNA90mer. Cells were harvested and cellular proteins were cross-linked with DNA. FLAG-tagged AIM2 and IFI16- $\beta$  proteins were immunoprecipitated. The bound DNA was purified and analyzed by PCR and qPCR. An enrichment of dsDNA90mer was found in the immunoprecipitated complexes containing FLAG-tagged AIM2 and IFI16- $\beta$  when compared with GFP (Fig 6D, top right panel, lanes 2 and 3 compared to 1). When increasing amount of V5-tagged IFI16- $\beta$  was co-expressed with fixed amount of FLAG-tagged AIM2, the levels of dsDNA90mer detected in the DNA–protein complex decreased (Fig 6D, lanes 4 and 5 compared to 3). Similar results were also obtained from qPCR analysis (Fig 6D, bottom right panel). These data were generally compatible with the competition of IFI16- $\beta$  with AIM2 for dsDNA binding. Our experiments corroborated with each other to indicate the ability of IFI16- $\beta$  to compete with AIM2 to suppress dsDNA sensing.

### IFI16- $\beta$ inhibits dsDNA-induced AIM2 inflammasome activation

The suppression of AIM2-ASC (Fig 5) and AIM2-dsDNA (Fig 6) interaction by IFI16- $\beta$  suggests that it might inhibit AIM2 inflammasome activation. To verify this, we reconstituted AIM2 inflammasome activation pathway in HEK293T cells by transiently overexpressing AIM2, ASC, procaspase-1, and pro-IL-1 $\beta$ . Cleavage of pro-IL-1 $\beta$  and secretion of mature IL-1 $\beta$  were monitored by

#### Figure 5. IFI16- $\beta$ interacts with AIM2 to impede AIM2-ASC complex formation.

- Domain structure of AIM2, p202, IFI16- $\alpha$ , and IFI16- $\beta$ . PYDs and the HIN domains (A, B or C) are indicated.
- IFI16- $\beta$  interacts with AIM2. A plasmid expressing FLAG-tagged AIM2 was co-transfected with IFI16- $\alpha$ -V5 or IFI16- $\beta$ -V5 plasmid into HEK293T cells. After 48 h, cells were harvested and lysed. Immunoprecipitation (IP) was carried out with mouse anti-FLAG antibody. Input proteins were analyzed by immunoblotting with mouse anti-FLAG or anti-V5 antibody. Immunoprecipitates were probed with rabbit anti-FLAG or anti-V5 antibodies.
- IFI16 HIN domains, but not PYD, are required for interaction with AIM2. AIM2-V5 plasmid was co-transfected with IFI16- $\alpha$ -FLAG, IFI16- $\beta$ -FLAG, or IFI16 PYD-FLAG construct into HEK293T cells. After 48 h, cells were harvested and lysed. Co-immunoprecipitation was carried out with mouse anti-V5 antibody. Input proteins were analyzed by immunoblotting with mouse anti-FLAG. Immunoprecipitates were probed with rabbit anti-V5 antibodies.
- Overexpression of IFI16- $\beta$  inhibits AIM2-ASC complex formation in HEK293T cells. Cells were co-transfected with the indicated combinations of expression plasmids for AIM2-V5, ASC-HA, IFI16- $\beta$ -FLAG, and p202-FLAG. After 48 h, cells were harvested and lysed. Immunoprecipitation was carried out with mouse anti-V5 antibody. Input proteins were analyzed by immunoblotting with mouse anti-FLAG, anti-HA, or anti-V5 antibody. Immunoprecipitates were probed with rabbit anti-FLAG, anti-HA, or anti-FLAG antibodies.
- Interaction between endogenous IFI16- $\beta$  and AIM2 proteins in THP-1-derived macrophages. THP-1 cells were differentiated into macrophages by overnight treatment with TPA (200 nM). Cells were harvested for cytosolic and nuclear fractionation. Immunoprecipitation was performed using mouse anti-IFI16C or anti-AIM2 antibody. Mouse anti-HA served as a control. The immune complexes were detected by immunoblotting with rabbit anti-IFI16N or anti-AIM2 antibodies.
- Association of IFI16- $\beta$  with endogenous AIM2 in HeLa cells. HeLa cells were transfected with the indicated combinations of plasmids expressing IFI16- $\alpha$ -FLAG, IFI16- $\beta$ -FLAG, and GFP-FLAG. Cells were then stimulated with IFN- $\beta$  (1,000 U/ml) to induce endogenous AIM2 expression. After 48 h, cells were harvested and lysed. Immunoprecipitation was carried out with mouse anti-FLAG or anti-AIM2 antibody. Immunoprecipitates were probed with rabbit anti-FLAG or anti-AIM2 antibodies.
- Overexpression of IFI16- $\beta$  impedes AIM2-ASC complex formation in THP-1 cells. Cells were transfected with increasing doses of IFI16- $\alpha$ -FLAG, IFI16- $\beta$ -FLAG, or GFP-FLAG plasmids. After 24 h, cells were differentiated into macrophages by overnight treatment with TPA (200 nM). Cells were then harvested and lysed. Endogenous AIM2 was immunoprecipitated using mouse anti-AIM2 antibody. The immune complexes were probed with rabbit anti-ASC or anti-AIM2 antibodies.

Data information: Three independent experiments were carried out with similar results.

Source data are available online for this figure.



immunoblotting. The amount of IL-1 $\beta$  protein in the culture supernatant was also measured by ELISA. Detection of IL-1 $\beta$  in the lysate and supernatant of AIM2-expressing cells confirmed that the reconstitution was successful (Fig 7A, lane 2 compared to 1). When we increased the expression of IFI16- $\beta$  in this system, AIM2-induced pro-IL-1 $\beta$  cleavage and IL-1 $\beta$  secretion as shown by immunoblotting and ELISA were dampened (Fig 7A, lanes 3 and 4 compared to 2). Furthermore, analysis of pro-IL-1 $\beta$  cleavage using the pro-IL-1 $\beta$ -Gaussia luciferase (iGluc) reporter assay, in which inflammasome activation can be measured by luciferase activity [48], revealed that overexpression of IFI16- $\beta$  specifically inhibited AIM2- but not NLRP3-induced inflammasome activation in HEK293T cells (Fig 7B).

To verify our findings obtained in the above surrogate models, inflammasome activation was further studied in differentiated THP-1 cells, which have been widely used to study AIM2 activity [5,6]. AIM2 and IFI16- $\beta$  proteins were expressed in THP-1 cells, which were subsequently differentiated into macrophages with TPA and further transfected with dsDNA90mer. This resulted in IL-1 $\beta$  secretion as detected by ELISA and immunoblot analysis of culture supernatant (Fig 7C). To confirm the role of AIM2 in dsDNA-induced inflammasome activation in these cells, we employed specific AIM2 and NLRP3 inflammasome inhibitors ODN-A151 and MCC950, respectively [49,50]. Indeed, whereas ODN-A151 was fully competent in the suppression of IL-1 $\beta$  secretion induced by dsDNA90mer, MCC950 exhibited no suppressive effect (Appendix Fig S2A). In contrast, inflammasome activation by nigericin was totally dependent on NLRP3 but not AIM2 (Appendix Fig S2B). Accordingly, knockdown of AIM2 or either isoform of IFI16 had no influence on nigericin-induced IL-1 $\beta$  secretion (Appendix Fig S2C). These results validated the use of differentiated THP-1 cells for the study of AIM2 inflammasome activation. Whereas overexpression of AIM2 further enhanced dsDNA90mer-induced IL-1 $\beta$  secretion in these cells, overexpression of IFI16- $\beta$  mitigated basal and AIM2-dependent secretion of IL-1 $\beta$  (Fig 7C). Thus, IFI16- $\beta$  inhibited AIM2 inflammasome activation in differentiated THP-1 cells.

To establish the physiological role of endogenous IFI16- $\beta$  in AIM2 inflammasome activation, loss-of-function experiments were

also performed in differentiated THP-1 cells and human MDMs. Two independent siRNAs specifically targeting IFI16- $\beta$  (siIFI16- $\beta$ 1 and siIFI16- $\beta$ 2) were employed to silence the expression of endogenous IFI16- $\beta$  in differentiated THP-1 cells. The effectiveness of these two siRNAs to deplete endogenous IFI16- $\beta$  expression at both mRNA and protein levels was verified. The silencing effect was highly specific since only IFI16- $\beta$  was affected but the levels of IFI16- $\alpha$  mRNA and protein remained unchanged (Fig 1F and Appendix Fig S3A). For comparison, siRNAs specifically targeting IFI16- $\alpha$  and AIM2 were included as controls. When AIM2 was knocked down in differentiated THP-1 cells, IL-1 $\beta$  and IL-18 secretion in response to dsDNA90mer, VACV70mer, nelfinavir, and infection with *Listeria monocytogenes* was blunted. However, the secretion was unaffected when cells were transfected with poly (I:C) or infected with VSV-GFP or HSV-1-GFP (Fig 8). These results were generally in keeping with previous reports on the requirement of AIM2 for inflammasome activation induced by dsDNA, nelfinavir, and *L. monocytogenes* [8,9,12,17,51]. Also consistent with previous publications [3,9,51], silencing of endogenous IFI16- $\alpha$  only affected IL-1 $\beta$  secretion triggered by HSV-1 infection but not by other stimuli tested. Of note, when endogenous IFI16- $\beta$  was depleted in differentiated THP-1 cells, the secretion of IL-1 $\beta$  and IL-18 induced by dsDNA90mer, VACV70mer, nelfinavir, or *L. monocytogenes* was augmented. In contrast, the depletion of IFI16- $\beta$  had no influence on IL-1 $\beta$  or IL-18 secretion induced by poly (I:C), VSV-GFP or HSV-1-GFP (Fig 8).

The controversy surrounding the role of AIM2 in inflammasome activation in human primary myeloid cells [4,11] prompted us to perform similar loss-of-function assays in human primary monocyte-derived macrophages (MDMs). As a first step, we confirmed that mRNA expression of AIM2, IFI16- $\alpha$ , and IFI16- $\beta$  could be specifically and effectively silenced in MDMs (Appendix Fig S3B). The cells were then primed with lipopolysaccharide (LPS) and stimulated with dsDNA90mer, poly (I:C), nelfinavir, or *L. monocytogenes*. Similar to results obtained in differentiated THP-1 cells, less IL-1 $\beta$  and IL-18 were detected in the culture supernatant of AIM2-knockdown human MDMs transfected with dsDNA90mer, treated with nelfinavir or infected with *L. monocytogenes*. In contrast, IFI16- $\beta$  knockdown in

#### Figure 6. IFI16- $\beta$ binds dsDNA to prevent it from binding to AIM2.

- IFI16- $\alpha$  and IFI16- $\beta$ , but not PYD, were pulled down by biotinylated dsDNA90mer (biotin-90mer). Plasmids expressing the indicated proteins were transfected into HEK293T. After 24 h, cells were further transfected with biotinylated dsDNA90mer. After another 3 hours, cells were lysed and biotin-DNA pull-down assay was carried out using streptavidin agarose.
- IFI16- $\beta$  and AIM2 were pulled down by biotinylated dsDNA90mer. The indicated proteins were overexpressed in HEK293T cells. After 24 h, biotinylated or non-biotinylated dsDNA90mer was delivered into cells. Three hours later, cells were lysed and biotin-DNA pull-down assay was carried out.
- IFI16- $\beta$  competes with AIM2 for dsDNA binding. HEK293T cells were transfected with plasmids expressing the indicated proteins. After 24 h, cells were further transfected with biotinylated dsDNA90mer. Three hours later, cells were harvested and lysed. Biotin-DNA pull-down assay was carried out by incubating 10  $\mu$ l streptavidin agarose with cell lysate for 3 h at 4°C. The agarose beads were washed five times with lysis buffer and then boiled in SDS-PAGE sample buffer. The precipitated proteins were visualized by immunoblotting with mouse anti-FLAG antibody.
- Binding of IFI16- $\beta$  and AIM2 with dsDNA90mer and inhibition of AIM2 binding with dsDNA90mer by IFI16- $\beta$ . HEK293T cells were transfected with plasmids expressing the indicated proteins. After 24 h, cells were further transfected with dsDNA90mer (1,000  $\mu$ g/ml). After another 3 h, cells were fixed for 5 min in 4% paraformaldehyde and quenched with 1 M Tris-Cl pH 7.4 for 5 min at room temperature. Fixed cells were washed with PBS and lysed in lysis buffer (50 mM Tris-Cl pH 7.4, 150 mM NaCl, 1 mM EDTA, 0.1% NP-40, and 1.25% Triton X-100). Immunoprecipitation was carried out with mouse anti-FLAG antibody at 4°C overnight. Immunoprecipitated complexes were washed five times with lysis buffer and then diluted in elution buffer (10 mM Tris-Cl, 1 mM EDTA and 0.65% SDS). To reverse the crosslinking, samples were incubated overnight at 65°C and then treated with 20  $\mu$ g/ml RNase A for 30 min at 37°C. Proteins were digested with 10  $\mu$ g/ml proteinase K for 2 h at 45°C. DNA was purified by Wizard<sup>®</sup> SV Gel and PCR Clean-Up System as per the manufacturer's instructions. The bound dsDNA90mer was detected by PCR and qPCR with previously described specific primers [62]. Three independent biological replicates were analyzed and error bars indicate SD. The differences between the indicated groups were statistically significant as judged by Student's *t*-test (\*\* $P$  < 0.01 and \*\*\* $P$  < 0.001).

Data information: Three independent experiments were performed with similar results.

Source data are available online for this figure.

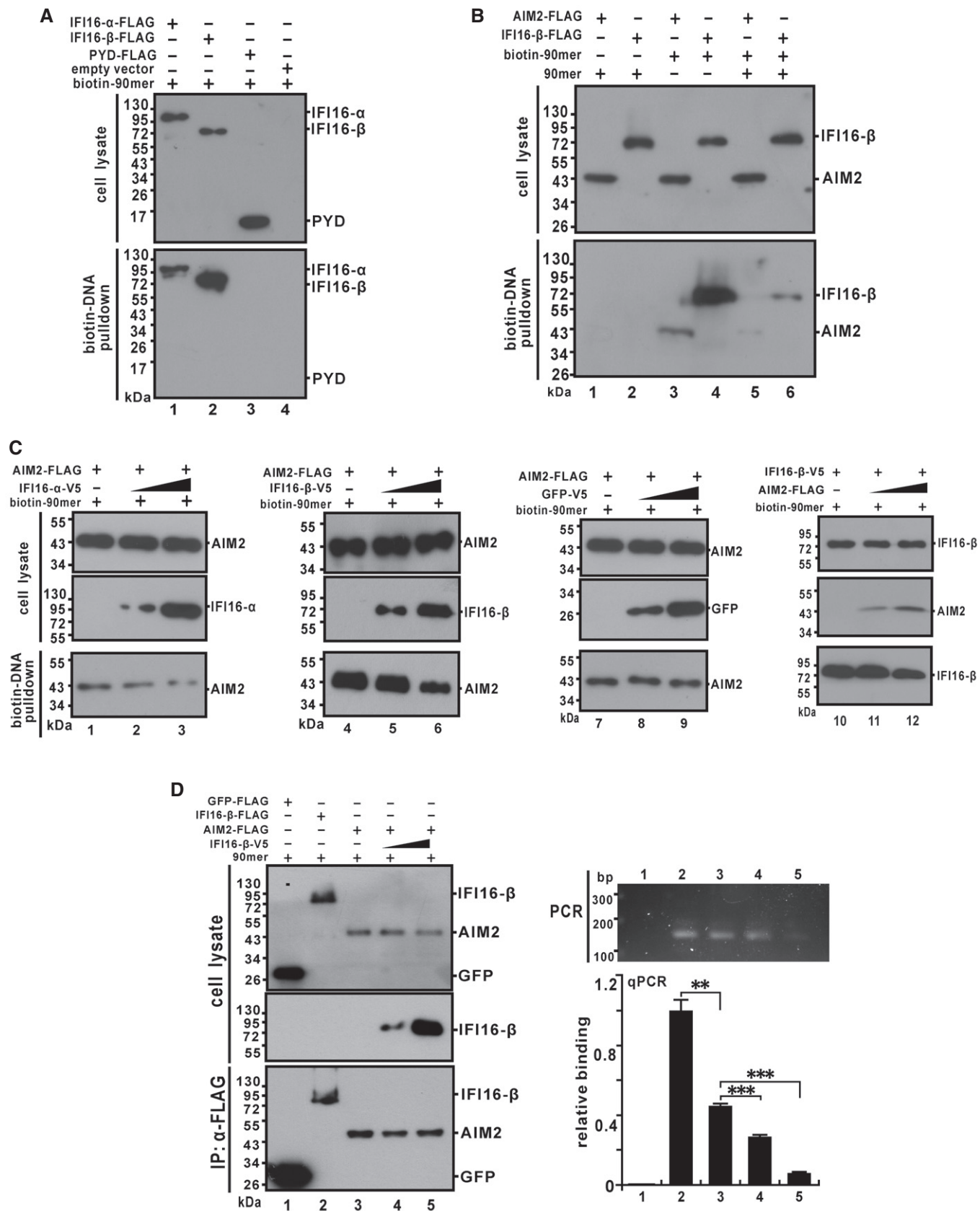
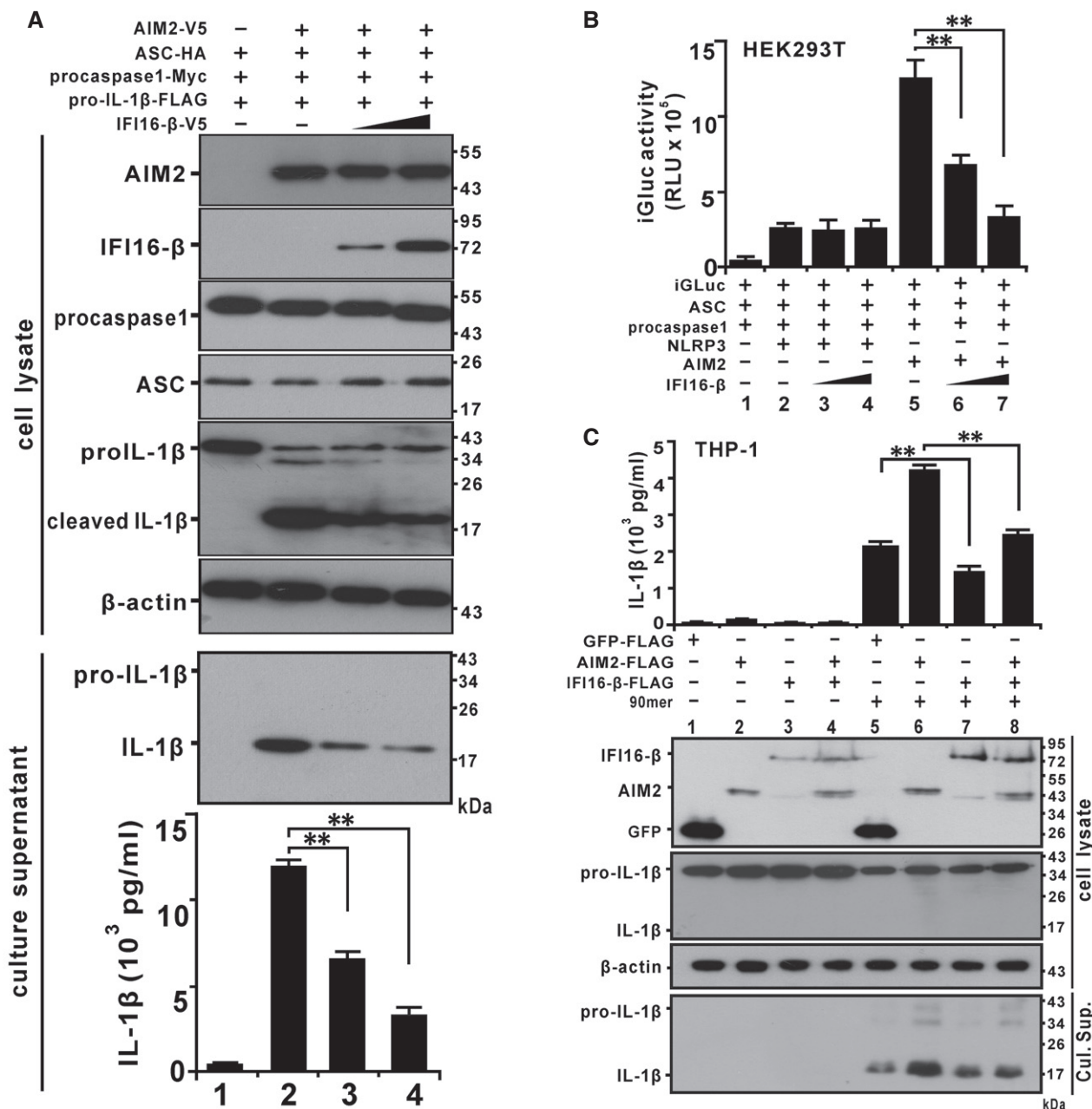


Figure 6.





**Figure 7. Overexpression of IFI16-β inhibits dsDNA-induced AIM2 inflammasome activation.**

**A** Reconstitution of AIM2 inflammasome activation in HEK293T cells by co-transfection of AIM2, ASC, procaspase-1, and pro-IL-1β plasmids. Mature IL-1β secreted into the culture supernatants was detected by immunoblotting and ELISA (\*\**P* < 0.01 by Student's *t*-test).

**B** HEK293T cells were transiently transfected with plasmids expressing iGLuc (50 ng), procaspase-1 (5 ng), ASC (5 ng), and either AIM2 (50 ng) or NLRP3 (50 ng). Increasing doses of IFI16-β plasmid (50 ng in lanes 3 and 6, and 150 ng in lanes 4 and 7) were co-transfected. Empty vector pcDNA6 was used to balance total amount of transfected DNA. Cell lysates were assessed 24 h after transfection for luciferase activity. RLU, relative luciferase unit (\*\**P* < 0.01 by Student's *t*-test).

**C** THP-1 cells were transfected with plasmids expressing the indicated proteins for 24 h and then differentiated by treatment with 10 nM TPA for 12 h. Cells were cultured with fresh medium without TPA for 12 h and transfected with dsDNA90mer (4.0 μg/ml). After another 12 h, cells were harvested for immunoblot analysis and the culture supernatants were collected for the detection of mature IL-1β secretion by ELISA (\*\**P* < 0.01 by Student's *t*-test).

Data information: Three independent biological replicates were analyzed and error bars indicate SD. Source data are available online for this figure.

these cells potentiated IL-1β and IL-18 secretion under the same conditions. Neither AIM2 nor IFI16-β was influential on poly (I:C)-induced IL-1β and IL-18 secretion (Fig 9). Interestingly, the effect of IFI16-β

depletion was opposite to that of AIM2 suppression. Together, our results consistently demonstrated the inhibition of dsDNA-induced AIM2 inflammasome activation by IFI16-β.

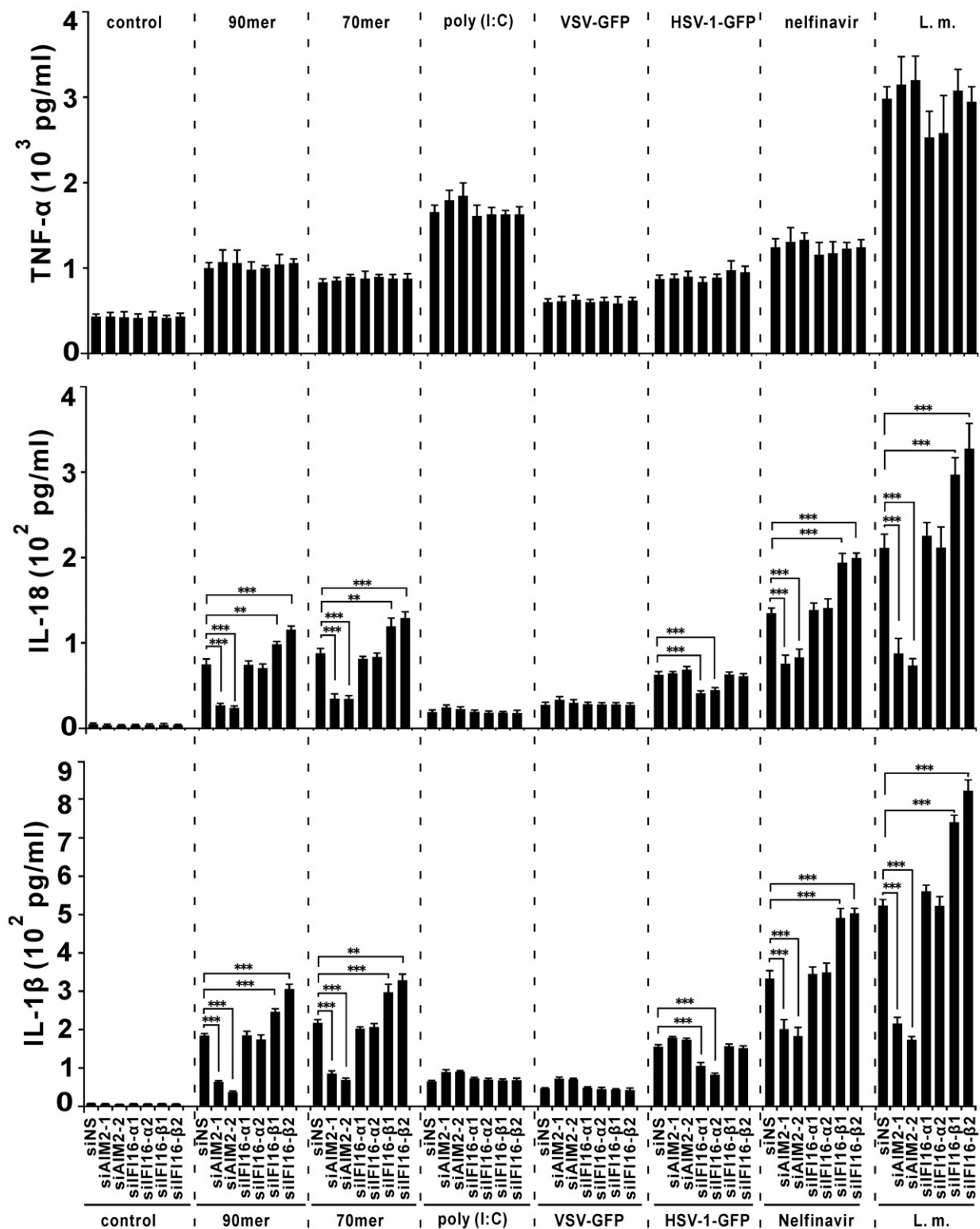


**Figure 8.** Knockdown of endogenous IFI16- $\beta$ , but not IFI16- $\alpha$  augmented cytoplasmic dsDNA-induced IL-1 $\beta$  and IL-18 secretion in differentiated THP-1 cells.

THP-1 cells were transfected with the indicated siRNA. After 12 h, THP-1 cells were differentiated into macrophages by treatment with 10 nM TPA for another 24 h. Cells were cultured for an additional 12 h without TPA. siRNA-transfected cells were further transfected with dsDNA90mer (4.0  $\mu$ g/ml), transfected with VACV70mer (4.0  $\mu$ g/ml), transfected with poly (I:C) (4.0  $\mu$ g/ml), infected with VSV-GFP (MOI = 0.01), infected with HSV-1-GFP (MOI = 5), exposed to nelfinavir (50  $\mu$ M), or infected with *Listeria monocytogenes* (L. m., MOI = 5). After another 12 h, culture supernatants were collected for the detection of mature TNF- $\alpha$ , IL-18, and IL-1 $\beta$  by ELISA. Three independent biological replicates were analyzed, and error bars indicate SD (\*\* $P$  < 0.01 and \*\*\* $P$  < 0.001 by Student's *t*-test).

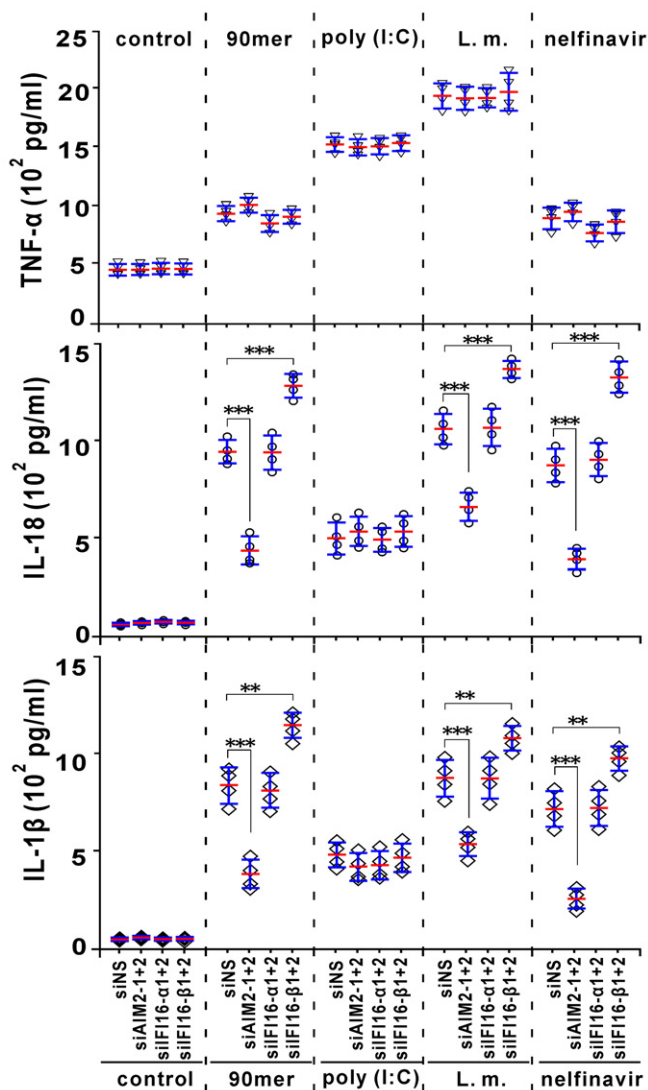


**Figure 9. Knockdown of endogenous IFI16-β, but not IFI16-α augmented cytoplasmic dsDNA-induced IL-1β and IL-18 secretion in human MDMs.**

Human MDMs ( $2.5 \times 10^5$ /ml) cultured in 24-well plates were repeatedly transfected with 0.5 μl of indicated siRNA for three times at 24-h intervals. After another 6 h, human MDMs were primed with LPS (1 μg/ml) for 6 h and then the culture medium was replaced with fresh RPMI1640. Two groups of cells were transfected twice with dsDNA90mer (4.0 μg/ml) and poly (I:C) (4.0 μg/ml), respectively, at 6-h intervals. The other two groups of cells were infected with *Listeria monocytogenes* (L.m., MOI = 5) or exposed to nelfinavir (50 μM) at 6 h after the change of medium. After another 12 h, culture supernatants were collected for detection of mature TNF-α, IL-18, and IL-1β by ELISA. Results were obtained from human MDMs derived from four different donors and presented as dot plots showing the distribution of data with the medians as well as upper and lower quartiles indicated by the three horizontal bars (\*\*P < 0.01 and \*\*\*P < 0.001 by Student's t-test). Two independent experiments were performed with similar results.

## Discussion

In this study, we have identified a novel transcript isoform of human IFI16-designated IFI16-β and provided multiple lines of evidence to support structural and functional similarities

between human IFI16-β and mouse p202. IFI16-β mRNA transcribed from an alternative promoter was widely expressed in different tissues and cells. Its expression was induced by IFN-β and other stimuli such as TPA. IFI16-β protein was translated and co-localized with AIM2 in the cytoplasm. IFI16-β also interacted with STING. Compared to IFI16-α, IFI16-β served as a weaker inducer of type I IFN production. More importantly, IFI16-β interacted with AIM2 and impeded its binding with ASC and dsDNA, leading to the inhibition of AIM2 inflammasome activation. Our findings revealed another level of negative regulation on AIM2 activity.

AIM2 is a key cytoplasmic DNA sensor that activates inflammasome [3]. Although DNA-induced inflammasome activation in human myeloid cells has recently been shown to be mediated through an AIM2-independent cGAS-STING-NLRP3 pathway [4], it is also well established that AIM2 is required for inflammasome activation in many physiological and pathological conditions such as infection with various DNA viruses including HSV-1, infection with bacteria including *L. monocytogenes* and disruption of nuclear integrity by nelfinavir [9–12]. Dysregulation of AIM2 inflammasome activation has been implicated in various diseases, such as vascular inflammation, psoriasis, pyogenic arthritis, pyoderma gangrenosum, and cryopyrin-associated periodic syndromes (CAPS) [50–52]. Mouse p202 has emerged as a major negative regulator of AIM2 but a similar human protein that contains HIN domains only has not been identified. Additional negative regulators of AIM2 such as Pypin-only proteins (POPs), CARD-only proteins (COPs), and TRIM11 have also been reported recently [52,53]. Particularly, POP1 and POP3 inhibit AIM2 inflammasome activation by interfering with PYD-PYD interaction [50,51]. These regulators might cooperate with each other to put AIM2 activation under control so that severe pathogenic inflammation will not be aggravated. A better understanding of the negative regulation of AIM2 inflammasome activation might reveal new strategies for anti-inflammatory therapy. In this regard, our demonstration of IFI16-β as a new inhibitor of AIM2 inflammasome activation might derive new knowledge for design and development of anti-inflammatory agents.

Mouse p202 negatively regulates AIM2 inflammasome activation through at least two mechanisms. On the one hand, p202 binds with dsDNA with higher affinity than AIM2 does [28–30]. On the other hand, p202 interacts with the HIN domains of AIM2 to prevent AIM2 oligomerization and ASC clustering [29,30]. In this study, we not only demonstrated structural similarity between IFI16-β and p202 but also obtained several lines of evidence to support that human IFI16-β is a functional homolog of mouse p202. First, IFI16-β binds dsDNA with higher affinity. Second, IFI16-β interacts with AIM2. Finally, IFI16-β functions as an inhibitor of dsDNA-induced AIM2 inflammasome activation. Given that mouse p202 is an SLE susceptibility locus [31] and IFI16-β was also upregulated in SLE patients, it would be of great interest to elucidate whether and how IFI16-β might contribute to SLE pathogenesis. p202 has previously been shown to be capable of translocating into the nucleus for the regulation of cell cycle and cellular response to growth factors through its direct interaction with transcription factors such as p53, NF-κB, AP1, and E2F [3]. Whether IFI16-β might serve similar function under physiological condition requires further investigations.

The biological function of IFI16- $\alpha$  as a DNA sensor to activate type I IFN production and to modulate inflammasome activation remains obscure. IFI16- $\alpha$  might sense replicating DNA of viruses in the nucleus leading to AIM2-independent activation of inflammasome [17,18,49]. Whether and how IFI16- $\beta$  might affect this process are not understood. Particularly, it will be of interest to see whether IFI16- $\beta$  might interact with IFI16- $\alpha$  and sequester it in the cytoplasm. In fact, IFI16- $\alpha$  has also been shown to interact with AIM2 in the cytoplasm and inhibit DNA-induced activation of AIM2 inflammasome [54]. Further analysis is required to clarify whether IFI16- $\beta$  might cooperate with IFI16- $\alpha$  to exert this function. Under some circumstances such as viral infection and inhibition of deacetylases, a portion of IFI16- $\alpha$  could translocate into the cytoplasm, bind with dsDNA using its HIN domains, and induce STING-dependent type I IFN expression [15,16,23,43]. Cooperation between IFI16- $\alpha$  and cGAS as well as potentiation of cGAMP production and function by IFI16- $\alpha$  has also been described [20,26]. IFI16- $\beta$  does not contain any NLS of IFI16- $\alpha$  and is therefore constitutively cytoplasmic. In our setting, IFI16- $\beta$  displayed a weak stimulatory effect on IFN- $\beta$  production. Exactly how this weak IFN-inducing activity might be achieved remains to be determined. The phenotype of mice deficient of all 13 AIM2-like PYHIN proteins indicated that p202 might not be absolutely required for DNA-induced type I IFN production [27]. However, currently we could not exclude the possibility that the lack of influence on DNA-induced IFN expression in these mutant mice might be attributed to simultaneous deletion of multiple positive and negative regulators [55]. In addition to AIM2 and IFI16- $\alpha$ , whether IFI16- $\beta$  might interact with other human PYHIN proteins IFIX and MNDA to modulate their activity merits further analysis.

In our study, IFI16- $\beta$  was shown to interact with STING, AIM2, and dsDNA. As discussed above, the impact of IFI16- $\beta$  on AIM2 inflammasome activity is likely attributed at least in part to its interaction with AIM2 and dsDNA. Our results are also consistent with the notion that IFI16- $\beta$  is influential on AIM2-dependent and NLRP3-independent inflammasome activation in our experimental setting. Whether the weak type I IFN-inducing activity of IFI16- $\beta$  might be ascribed to its interaction with STING, cGAS, or IFI16- $\alpha$  requires further exploration.

Several additional functions of IFI16- $\alpha$  unrelated to innate immune response have also been described [56]. IFI16- $\alpha$  restricts HSV-1 and HCMV replication by preventing the transcription of viral genes [19,57,58]. IFI16- $\alpha$  also inhibits human papillomavirus 18 transcription through epigenetic modification of viral promoters [59]. In addition, IFI16- $\alpha$  interacts with p53 and BRCA1 to modulate transcription and DNA repair [18,56]. Given that IFI16- $\beta$  has the same HIN A and HIN B domains as IFI16- $\alpha$ , it will be of interest to determine whether IFI16- $\beta$  might also be involved in these processes.

We also noticed that the expression level of IFI16- $\beta$  was much lower than that of IFI16- $\alpha$  in resting and stimulated THP-1 cells. Despite this, IFI16- $\beta$  was still able to inhibit dsDNA-induced activation of AIM2 inflammasome. In addition, dose-dependent inhibition of AIM2 inflammasome activation by IFI16- $\beta$  was also observed. Notably, the expression level of p202 is very low and it is even barely detectable in some mouse strains such as C57BL/6 [14,28]. p202 and IFI16- $\beta$  not only inhibit AIM2 activity through effective competition for dsDNA binding but they can also create steric hindrance to impede AIM2 oligomerization [29,30]. Plausibly, one

molecule of p202 or IFI16- $\beta$  was capable of perturbing the formation of a large multi-subunit inflammasome complex [28]. Thus, the inhibitory effect of p202 and IFI16- $\beta$  on AIM2 activity could be amplified [29,30,50]. The low expression level of IFI16- $\beta$  in resting cells may ensure that the acute phase of host defense would not be affected. However, IFI16- $\beta$  was induced by IFN- $\beta$  and other stimuli such as TPA. This might therefore contribute to the brake of inflammasome activation during the resolution phase of inflammation following viral or bacterial infection. Some of these issues might be clarified by specific knockout of IFI16- $\beta$  in human cells and animal models.

## Materials and Methods

### Cell culture and transfection

HEK293, HEK293T, HeLa, MCR-5, IMR90, LX-2, MDA-MB-231, WI38, HCT116, U2OS, A549, BEL-7402, Hep3B, and Vero cells were cultured in Dulbecco's modified Eagle's medium (DMEM) (Life Technologies, New York, USA) with 10% heat-inactivated fetal bovine serum (FBS) (Life Technologies) as previously described [60,61]. CEM-T4, MT2, Jurkat, THP-1, U937, and HuT102 were cultured in RPMI1640 medium (Life Technologies) with 10% heat-inactivated FBS. These cells were maintained by the addition of fresh medium or replacement of medium at a cell concentration between  $5 \times 10^4$  and  $2 \times 10^6$  cells/ml. HepG2 was cultured in Earle's minimum essential medium (EMEM) with 10% heat-inactivated FBS. Plasmid DNA was transfected into HEK293, HEK293T, and HeLa cells using GeneJuice<sup>®</sup> Transfection Reagent (Novagen, Sydney, Australia).

### Plasmids

cDNAs of human IFI16 (IMAGE 3914632) and mouse p202 (IMAGE 4945964) were obtained from Source BioScience (Nottingham, UK). The open reading frames (ORFs) of AIM2 and IFI16- $\beta$  were amplified from reverse-transcribed cDNA from IFN- $\beta$ -stimulated THP-1 cells. Expression plasmids for human pro-IL-1 $\beta$  and ASC were kindly provided by Pascal Schneider (University of Lausanne, Switzerland). Expression plasmid for human procaspase 1 was a gift from Guy Salvesen (Sanford Burnham Prebys Medical Discovery Institute, La Jolla, California, USA). The ORFs of these genes were subcloned into pcDNA6B (Invitrogen, USA) or pCAGEN mammalian expression vectors with different C-terminal tags. Expression plasmids pcDNA6B-hSTING-HA, pcDNA6B-mSTING-HA, and pCAGEN-cGAS have been described elsewhere [46]. pCAGEN was a gift from Connie Cepko (Harvard Medical School, USA). For subcellular localization, eGFP was inserted into Xba I and Sac II restriction sites of pcDNA6B to construct pcDNA6B-eGFP vector, into which IFI16- $\alpha$  and IFI16- $\beta$  genes were subcloned. Promoter regions of IFI16- $\alpha$  and IFI16- $\beta$  were amplified from genomic DNA of HeLa cells and cloned into the firefly luciferase reporter plasmid pGL3-Basic (Promega, USA) as previously described [46,61]. pcDNA6B-IFI16- $\alpha$  $\Delta$ NLS1-eGFP, pGL3-IFI16- $\alpha$  $\Delta$ -luc, and pGL3-IFI16- $\beta$  $\Delta$ -luc mutants were constructed using the QuikChange II XL Site-Directed Mutagenesis Kit (Agilent Technologies, USA). All plasmids were verified by DNA sequencing. Primers used for plasmid construction were listed in Appendix Table S1.



### Nucleic acids and inflammasome inhibitors

Polyinosinic–polycytidylic acid [poly (I:C)] was purchased from Sigma, USA (Cat #: P1530). AIM2 inflammasome inhibitor ODN-A151 (Cat #: tlr1-ttag151) and NLRP3 inflammasome inhibitor MCC950 (Cat #: inh-mcc) were purchased from InvivoGen, USA. Nelfinavir mesylate was bought from Sigma (Cat #: PZ0013). dsDNA90mer, a dsDNA of 90 bp derived from HSV-1 genome [62], was obtained by annealing two DNA oligonucleotides 5'-TACA GATCTACTAGTGATCTATGACTGATCTGTACATGATCTACATACA GATCTACTAGTGATCTATGACTGATCTGTACATGATCTACA-3' (forward) and 5'-TACAGATCTACTAGTGATC TATGACTGATCTGTACATGATCTACATACAGATCTACTAGTGATCTATGACTGATCTGTACATGATCTACA-3' (reverse). 5'-biotinylated dsDNA90mer was prepared as described [62]. VACV70mer is another dsDNA of 70 bp derived from VACV genome [15]. VACV70mer was generated by annealing 5'-CCATCAGAAAGAGGTTTAAATTTTTGTGAGACCATC GAAGAG AGAAAGAGATAAACTTTTTTACGACT-3' (forward) and 5'-AGTCGTAAGAAAAGTTTATCT CTTTCTCTCTCGATGGTCTCA CAAAAATATTAACCTCTTCTGATGG-3' (reverse). DNA oligonucleotides were synthesized by Integrated DNA Technologies (Singapore).

### Immunoblotting and antibodies

Cells were lysed by sonication in RIPA-150 buffer (50 mM Tris–Cl, pH 7.4, 150 mM NaCl, 1% Triton X-100, 0.1% SDS, 1% sodium deoxycholate, 1% NP-40, and 0.5 mM EDTA) supplemented with 1 $\times$  protease inhibitor cocktail (Roche, Germany). Protein concentrations of cell lysates were determined by Bradford reagent (Bio-Rad, USA). Total proteins were resolved by SDS–PAGE. Gels were transferred to PVDF membranes and immunoblotted using the protocols recommended by the manufacturer. Proteins were visualized by a chemiluminescent reagent WesternBright™ ECL (Advansta, USA) as described previously [46,60,61]. Primary antibodies used were mouse anti-IFI16C (1:1,000 dilution; ab50004 from Abcam, USA), rabbit anti-IFI16C (1:1,000 dilution; 14970 from Cell Signaling, USA), mouse anti-IFI16N (1:500 dilution; sc-8023 from Santa Cruz, USA), mouse anti-AIM2 (1:1,000 dilution; 3B10 from BioLegend, USA), rabbit anti-AIM2 (1:1,000 dilution; ab180665 from Abcam), mouse anti-FLAG (M2) (1:5,000 dilution; F1804 from Sigma), mouse anti-V5 (1:5,000 dilution; R960CUS from Invitrogen), mouse anti-c-Myc (1:1,000 dilution; 9E10 from Santa Cruz), mouse anti- $\beta$ -actin (1:5,000 dilution; AC-15 from Sigma), rabbit anti-cleaved-IL-1 $\beta$  (1:200 dilution; Cell Signaling) for detection of secreted IL-1 $\beta$  in culture supernatant, and rabbit anti-pro-IL-1 $\beta$  (1:1,000 dilution; Cell Signaling) for detection of pro-IL-1 $\beta$  in cell lysates. Horseradish peroxidase-conjugated secondary antibodies were goat anti-rabbit (1:5,000 dilution; RPN4301 from GE Healthcare, USA) and sheep anti-mouse (1:5,000 dilution; NA931 from GE Healthcare). Fluorescent secondary antibodies were tetramethylrhodamine-labeled goat anti-mouse IgG (1:200 dilution; Zymed, USA) and fluorescein-labeled goat anti-rabbit IgG (1:500 dilution; Invitrogen).

### Human peripheral blood samples

Peripheral blood samples were collected from 24 Chinese patients with SLE and 24 healthy Chinese blood donors. Diagnosis of SLE

was based on the American College of Rheumatology-endorsed criteria sets for classification of SLE as detailed in our previous publications [63]. All blood samples were collected from Queen Mary Hospital in Hong Kong. Total mRNA was extracted from PBMCs and then reverse-transcribed into cDNA as described [63]. The protocol for blood collection was reviewed and approved by the Joint Institutional Review Board of the University of Hong Kong and Hospital Authority Hong Kong West Cluster.

### Human MDMs

Healthy adult blood samples were obtained from Hong Kong Red Cross Blood Transfusion Service according to a protocol approved by the Joint Institutional Review Board of the University of Hong Kong and Hospital Authority Hong Kong West Cluster. Human peripheral blood samples were obtained from healthy donors. Peripheral blood mononuclear cells (PBMCs) were isolated by density gradient centrifugation (750 g for 20 min at 18°C) through Ficoll-Paque Plus (GE Healthcare). The major band undisturbed at the interphase containing PBMCs was harvested. After three washes with PBS, PBMCs were cultured with RPMI1640 containing 10% FBS for 1 h and then the non-adherent lymphocytes were removed. Human MDMs were obtained by culturing the adherent monocytes with RPMI1640 containing 10% FBS, 1% penicillin–streptomycin, 1% MEM non-essential amino acids solution (Life Technologies), 1 mM sodium pyruvate, and 20 ng/ml granulocyte–macrophage colony-stimulating factor (Abcam) for 7 days before experiments.

### Cell fractionation

Cytosolic and nuclear extracts were isolated using NE-PER™ Nuclear and Cytoplasmic Extraction Reagents (Thermo Fisher, USA) as per the manufacturer's instructions. The purity of cytosolic and nuclear extracts was assessed by immunoblotting with anti-GAPDH and anti-histone 4 (Merck, USA) antibodies, respectively.

### Co-immunoprecipitation

Cells were lysed in RIPA-150 buffer containing 1 $\times$  protease inhibitor cocktail. Cell lysate supernatants were incubated with antibodies for 2 h. rProtein G agarose (Invitrogen) was then added into the mixture to incubate for another 18 h at 4°C. Beads were washed 3–5 times with RIPA-150 or RIPA-250 (50 mM Tris–Cl, pH 7.4, 250 mM NaCl, 1% Triton X-100, 0.1% SDS, 1% sodium deoxycholate, 1% NP-40, and 0.5 mM EDTA) buffer. After extensive washing, the immunoprecipitates were eluted with 1 $\times$  SDS–PAGE sample buffer by boiling for 5 min. The input and output samples were applied to SDS–PAGE and analyzed by immunoblotting.

### Biotin–DNA pull-down

Biotin–DNA pull-down was performed as described [62]. Twenty-four hours after plasmid transfection, biotinylated or non-biotinylated dsDNA90mer was further transfected into HEK293T cells with Lipofectamine 2000 (Invitrogen). After another 3 h, cells were harvested and lysed by sonication in RIPA-150 buffer. Supernatants were incubated with streptavidin agarose (Invitrogen) for 3 h, and beads were washed five times with RIPA-150 or RIPA-250 buffer.

After washing, beads were re-suspended in 1 $\times$  SDS–PAGE sample buffer and boiled for 5 min. Precipitated proteins were visualized by immunoblotting with mouse anti-FLAG antibody.

### Protein–dsDNA co-immunoprecipitation

Protein–dsDNA co-immunoprecipitation was performed as described [15,62]. Twenty-four hours after plasmid transfection, dsDNA90mer was further transfected into HEK293T cells with Lipofectamine 2000. After 1 h, cells were harvested and fixed for 10 min in 4% paraformaldehyde. After quenching with 1 M Tris–Cl (pH 7.4) for 5 min, cell pellets were washed three times with cold PBS and then lysed with RIPA-150 buffer containing 1 $\times$  protease inhibitor cocktail. FLAG-tagged proteins were immunoprecipitated as described above. The sample was separated into two tubes. One tube containing 1/4 volume of the total sample was boiled with SDS–PAGE sample buffer to elute the precipitated proteins for subsequent immunoblot analysis. The other tube containing 3/4 volume of the total sample was incubated overnight at 65°C to reverse crosslinking. Samples were treated with 20  $\mu$ g/ml RNase A (Invitrogen) at 37°C for 30 min and then with 10  $\mu$ g/ml proteinase K (Sigma) at 37°C for 2 h. Bound DNA was purified using the Wizard SV Gel & PCR Clean-Up System (Promega). Purified DNA was further analyzed by RT–PCR and qPCR.

### Viruses

SeV Cantell strain was bought from American Type Culture Collection (ATCC; Manassas, Virginia, USA). VSV-GFP and HSV-1-GFP were propagated and quantified as detailed in our previous publications [60,64]. ICP0-null HSV-1 virus (HSV-1-ICP0) was a gift from David Knipe (Harvard Medical School) [40]. In this study, SeV, VSV-GFP, HSV-1-GFP, and HSV-1-ICP0 were used to infect human cell lines [54,55,58]. Briefly, before virus infection, cells were washed twice with pre-warmed serum-free medium at 37°C. Virus was diluted to the desired MOI with serum-free medium. Virus was incubated with cells for 1 h in a CO<sub>2</sub> incubator. Fresh culture medium was added at the end of the infection.

### *Listeria monocytogenes*

*Listeria monocytogenes* EGD (serovar 1/2a) strain, which has been shown to activate AIM2 inflammasome [8], was a gift from Da-Hai Yang and Gabriel Núñez (University of Michigan, USA). *Listeria monocytogenes* was cultured in brain–heart infusion (BHI) broth overnight at 37°C with shaking. It was then diluted 100-fold with fresh BHI broth and incubated at 37°C with shaking until an OD<sub>600</sub> of 0.8 was reached. *L. monocytogenes* cells were harvested by centrifugation, washed with PBS, and serially diluted on BHI agar plates.

### Confocal immunofluorescence microscopy

HeLa cells were plated on glass coverslips and grown to 50% confluence. Cells were transfected and then fixed with 4% paraformaldehyde for 15 min. The subcellular localization of IFI16- $\alpha$ -eGFP and IFI16- $\beta$ -eGFP was observed directly under confocal microscope. THP-1 cells were transfected with pcDNA6B-IFI16- $\beta$ -FLAG, plated on glass coverslips, and then differentiated into macrophages by treatment with 200 nM TPA for 24 h. To stain for

AIM2-V5 and STING-HA in HeLa cells or IFI16- $\beta$ -FLAG in THP-1-derived macrophages, cells were fixed and then permeabilized in PBS containing 0.1% (v/v) Triton X-100 (PBST) for 5 min, blocked with 5% bovine serum albumin in PBST for 1 h, and reacted with mouse anti-V5, anti-HA, or anti-FLAG antibody overnight at 4°C. Endogenous AIM2 was stained with rabbit anti-AIM2 (Abcam). Cells were washed extensively with PBST, incubated with fluorescent secondary antibodies for 1 h at room temperature, and washed three times with PBST. Coverslips were then stained with DAPI (blue), mounted onto the slides, and imaged using Carl Zeiss LSM710 microscope as described previously [60].

### Transfection and stimulation of THP-1 cells

siRNA and synthetic dsDNA were transfected into THP-1 cells using Lipofectamine 2000 (Invitrogen) according to the manufacturer's instructions and as described previously [60,61]. Plasmid DNA was transfected into THP-1 cells with GeneXplus Transfection Reagent (ACS-4004™ from ATCC). Twelve hours after transfection, THP-1 cells were differentiated to macrophages by treating with 10 nM TPA (Cell Signaling) for 24 h. Cells were cultured for an additional 12 h in the absence of TPA and then stimulated for 12 h either with synthetic dsDNA (4.0  $\mu$ g/ml) and poly (I:C) (4.0  $\mu$ g/ml) transfected into cells with Lipofectamine 2000 or with viral infection as described above. siRNA was transfected into human MDMs using Lipofectamine® RNAiMAX Reagent (Invitrogen) according to the manufacturer's instructions. Synthetic dsDNA and poly (I:C) were transfected into human MDMs with Lipofectamine 3000 (Invitrogen), and the transfection was repeated 6 h later using Lipofectamine 2000 (Invitrogen). Culture supernatants were collected for measurement of secreted cytokines. Cells were harvested for subsequent analysis. All siRNAs were designed using Stealth™ RNAi method (Invitrogen) and synthesized by GenePharma (Shanghai, China). The non-silencing siRNA (siNS) was provided by GenePharma. siRNA sequences were listed in Appendix Table S2.

### Real-time RT–qPCR

Total RNA was isolated with TRIzol Reagent (Invitrogen) as per the manufacturer's instructions. RNA was reverse-transcribed into cDNA with Transcriptor First Strand cDNA Synthesis Kit (Roche). RT–qPCRs and analysis were performed using Applied Biosystems StepOnePlus™ Real-Time PCR System as described [60, 61]. SYBR Premix Ex Taq kit (Takara Bio, Dalian, China) was used for SYBR Green-based RT–qPCR according to the manufacturer's protocol. Reference was made to GAPDH mRNA. Comparative C<sub>T</sub> method ( $\Delta\Delta C_T$  method) was used for the calculation of fold change in gene expression.

### ELISA

The concentration of secreted IL-1 $\beta$  in culture supernatants was measured by human IL-1 $\beta$  ELISA Kit (ADI-900-130, Enzo Life Sciences Assay Designs Inc., USA) according to the manufacturer's instructions. Briefly, serially diluted IL-1 $\beta$  standards provided in the kit and samples for detection were incubated in the pre-coated wells for 1 h, washed with the washing buffer, and probed with anti-IL-1 $\beta$  antibody for 1 h. The wells were washed, incubated with HRP-tagged

antibodies for 3 h, washed again, and incubated with substrate for 30 min. The reaction was terminated with a stop solution. After 5 min, readings were taken at 450 nm and protein concentrations were calculated based on a standard curve. TNF- $\alpha$  and IL-18 were detected by ELISA kits from R&D Systems, USA (Cat #: DY210 and DY318).

### Luciferase reporter assays

Dual-luciferase reporter assay was performed using the protocol and reagents provided by Promega, USA, as previously described [46,61]. All reporter constructs including IFN- $\beta$ -luc, IRF3-luc, and ISRE-luc have been detailed elsewhere [60,61]. Cell lysates were loaded into a 96-well plate for measurement of luciferase activity in a Microplate luminometer LB 96V (EG&G Berthold, Germany). Normalization of transfection efficiency was achieved by co-transfection of pRL-TK reporter (Promega). Relative luciferase activity was calculated by normalizing firefly luciferase activity to that of *Renilla* luciferase. Pro-IL-1 $\beta$ -Gaussia luciferase (iGLuc) is a luciferase-based reporter system for inflammasome activity [48]. iGLuc plasmid was provided by Veit Hornung (University of Bonn, Germany). iGLuc-based luciferase activity was measured using the Pierce Gaussia Luciferase Glow Assay kit (Thermo Fisher).

### Statistical analysis

Two-tailed unpaired Student's *t*-tests were used for statistical analysis by GraphPad Prism 5.0 and Microsoft Excel. All results are representative of at least three independent biological replicates and expressed as mean values  $\pm$  SD. In all cases, differences were considered to be statistically significant at  $P < 0.05$ .

**Expanded View** for this article is available online.

### Acknowledgements

We thank Connie Cepko, Dominique Garcin, Veit Hornung, David Knipe, Brian Lichty, Ian Mohr, Gabriel Núñez, Jacques Perrault, Guy Salvesen, Pascal Schneider, and Da-Hai Yang for reagents. We also thank Xiao-Qiang Yu, Pak-Yin Lui, Hinson Cheung, and Isaac Lui for critical reading of manuscript. The work was supported in part by Hong Kong Health and Medical Research Fund (HKM-15-M01 and 15140682) and Hong Kong Research Grants Council (HKU171091/14M and C7011-15R).

### Author contributions

P-HW and D-YJ conceptualized and designed the study. Chi-PC and K-HK provided expert advice and crucial support to D-YJ. P-HW performed all experiments with the help from Z-WY, J-JD, K-LS, W-WG, VC, YC, S-YF, K-SY, T-HH, C-PC, YZ, and WY. YZ and WY provided SLE patient samples and advice. All authors contributed to data analysis. P-HW and D-YJ wrote the manuscript with input from all authors.

### Conflict of interest

The authors declare that they have no conflict of interest.

## References

- Paludan SR, Bowie AG (2013) Immune sensing of DNA. *Immunity* 38: 870–880

- Sun L, Wu J, Du F, Chen X, Chen ZJ (2013) Cyclic GMP-AMP synthase is a cytosolic DNA sensor that activates the type I interferon pathway. *Science* 339: 786–791
- Schattgen SA, Fitzgerald KA (2011) The PYHIN protein family as mediators of host defenses. *Immunol Rev* 243: 109–118
- Gaidt MM, Ebert TS, Chauhan D, Ramshorn K, Pinci F, Zuber S, O'Duill F, Schmid-Burgk JL, Hoss F, Buhmann R et al (2017) The DNA inflammasome in human myeloid cells is initiated by a STING-cell death program upstream of NLRP3. *Cell* 171: 1110–1124
- Fernandes-Alnemri T, Yu JW, Datta P, Wu J, Alnemri ES (2009) AIM2 activates the inflammasome and cell death in response to cytoplasmic DNA. *Nature* 458: 509–513
- Hornung V, Ablasser A, Charrel-Dennis M, Bauernfeind F, Horvath G, Caffrey DR, Latz E, Fitzgerald KA (2009) AIM2 recognizes cytosolic dsDNA and forms a caspase-1-activating inflammasome with ASC. *Nature* 458: 514–518
- Jin T, Perry A, Jiang J, Smith P, Curry JA, Unterholzner L, Jiang Z, Horvath G, Rathinam VA, Johnstone RW et al (2012) Structures of the HIN domain: DNA complexes reveal ligand binding and activation mechanisms of the AIM2 inflammasome and IFI16 receptor. *Immunity* 36: 561–571
- Fernandes-Alnemri T, Yu JW, Juliana C, Solorzano L, Kang S, Wu J, Datta P, McCormick M, Huang L, McDermott E et al (2010) The AIM2 inflammasome is critical for innate immunity. *Nat Immunol* 11: 385–393
- Rathinam VA, Jiang Z, Waggoner SN, Sharma S, Cole LE, Waggoner L, Vanaja SK, Monks BG, Ganesan S, Latz E et al (2010) The AIM2 inflammasome is essential for host defense against cytosolic bacteria and DNA viruses. *Nat Immunol* 11: 395–402
- Burckstummer T, Baumann C, Bluml S, Dixit E, Durnberger G, Jahn H, Planyavsky M, Bilban M, Colinge J, Bennett KL et al (2009) An orthogonal proteomic-genomic screen identifies AIM2 as a cytoplasmic DNA sensor for the inflammasome. *Nat Immunol* 10: 266–272
- Lugrin J, Martinon F (2018) The AIM2 inflammasome: sensor of pathogens and cellular perturbations. *Immunol Rev* 281: 99–114
- Di Micco A, Frera G, Lugrin J, Jamilloux Y, Hsu ET, Tardivel A, De Gassart A, Zaffalon L, Bujisic B, Siegert S et al (2016) AIM2 inflammasome is activated by pharmacological disruption of nuclear envelope integrity. *Proc Natl Acad Sci USA* 113: E4671–E4680
- Brunette RL, Young JM, Whitley DG, Brodsky IE, Malik HS, Stetson DB (2012) Extensive evolutionary and functional diversity among mammalian AIM2-like receptors. *J Exp Med* 209: 1969–1983
- Cridland JA, Curley EZ, Wykes MN, Schroder K, Sweet MJ, Roberts TL, Ragan MA, Kassahn KS, Stacey KJ (2012) The mammalian PYHIN gene family: phylogeny, evolution and expression. *BMC Evol Biol* 12: 140
- Unterholzner L, Keating SE, Baran M, Horan KA, Jensen SB, Sharma S, Sirois CM, Jin T, Latz E, Xiao TS et al (2010) IFI16 is an innate immune sensor for intracellular DNA. *Nat Immunol* 11: 997–1004
- Li T, Diner BA, Chen J, Cristea IM (2012) Acetylation modulates cellular distribution and DNA sensing ability of interferon-inducible protein IFI16. *Proc Natl Acad Sci USA* 109: 10558–10563
- Kerur N, Veettil MV, Sharma-Walia N, Bottero V, Sadagopan S, Otageri P, Chandran B (2011) IFI16 acts as a nuclear pathogen sensor to induce the inflammasome in response to Kaposi Sarcoma-associated herpesvirus infection. *Cell Host Microbe* 9: 363–375
- Dutta D, Dutta S, Veettil MV, Roy A, Ansari MA, Iqbal J, Chikoti L, Kumar B, Johnson KE, Chandran B (2015) BRCA1 regulates IFI16 mediated nuclear innate sensing of herpes viral DNA and subsequent induction of the innate inflammasome and interferon- $\beta$  responses. *PLoS Pathog* 11: e1005030

19. Roy A, Dutta D, Iqbal J, Pisano G, Gjyshi O, Ansari MA, Kumar B, Chandran B (2016) Nuclear innate immune DNA sensor IFI16 is degraded during lytic reactivation of Kaposi's sarcoma-associated herpesvirus (KSHV): role of IFI16 in maintenance of KSHV latency. *J Virol* 90: 8822–8841
20. Jønsson KL, Laustsen A, Krapp C, Skipper KA, Thavachelvam K, Hotter D, Egedal JH, Kjolby M, Mohammadi P, Prabakaran T et al (2017) IFI16 is required for DNA sensing in human macrophages by promoting production and function of cGAMP. *Nat Commun* 8: 14391
21. Monroe KM, Yang Z, Johnson JR, Geng X, Doitsh G, Krogan NJ, Greene WC (2014) IFI16 DNA sensor is required for death of lymphoid CD4 T cells abortively infected with HIV. *Science* 343: 428–432
22. Munoz-Arias I, Doitsh G, Yang Z, Sowinski S, Ruelas D, Greene WC (2015) Blood-derived CD4 T cells naturally resist pyroptosis during abortive HIV-1 infection. *Cell Host Microbe* 18: 463–470
23. Ansari MA, Dutta S, Veetil MV, Dutta D, Iqbal J, Kumar B, Roy A, Chikoti L, Singh VV, Chandran B (2015) Herpesvirus genome recognition induced acetylation of nuclear IFI16 is essential for its cytoplasmic translocation, inflammasome and IFN- $\beta$  responses. *PLoS Pathog* 11: e1005019
24. Ghosh S, Wallerath C, Covarrubias S, Hornung V, Carpenter S, Fitzgerald KA (2017) The PYHIN protein p205 regulates the inflammasome by controlling Asc expression. *J Immunol* 199: 3249–3260
25. Diner BA, Lum KK, Toettcher JE, Cristea IM (2016) Viral DNA sensors IFI16 and cyclic GMP-AMP synthase possess distinct functions in regulating viral gene expression, immune defenses, and apoptotic responses during herpesvirus infection. *MBio* 7: e01553-16
26. Almine JF, O'Hare CA, Dunphy G, Haga IR, Naik RJ, Atrih A, Connolly DJ, Taylor J, Kelsall IR, Bowie AG et al (2017) IFI16 and cGAS cooperate in the activation of STING during DNA sensing in human keratinocytes. *Nat Commun* 8: 14392
27. Gray EE, Winship D, Snyder JM, Child SJ, Geballe AP, Stetson DB (2016) The AIM2-like receptors are dispensable for the interferon response to intracellular DNA. *Immunity* 45: 255–266
28. Roberts TL, Idris A, Dunn JA, Kelly GM, Burnton CM, Hodgson S, Hardy LL, Garceau V, Sweet MJ, Ross IL et al (2009) HIN-200 proteins regulate caspase activation in response to foreign cytoplasmic DNA. *Science* 323: 1057–1060
29. Ru H, Ni X, Zhao L, Crowley C, Ding W, Hung LW, Shaw N, Cheng G, Liu ZJ (2013) Structural basis for termination of AIM2-mediated signaling by p202. *Cell Res* 23: 855–858
30. Yin Q, Sester DP, Tian Y, Hsiao YS, Lu A, Cridland JA, Sagulenko V, Thygesen SJ, Choubey D, Hornung V et al (2013) Molecular mechanism for p202-mediated specific inhibition of AIM2 inflammasome activation. *Cell Rep* 4: 327–339
31. Rozzo SJ, Allard JD, Choubey D, Vyse TJ, Izui S, Peltz G, Kotzin BL (2001) Evidence for an interferon-inducible gene, Ifi202, in the susceptibility to systemic lupus. *Immunity* 15: 435–443
32. Panchanathan R, Duan X, Shen H, Rathinam VA, Erickson LD, Fitzgerald KA, Choubey D (2010) Aim2 deficiency stimulates the expression of IFN-inducible Ifi202, a lupus susceptibility murine gene within the Nba2 autoimmune susceptibility locus. *J Immunol* 185: 7385–7393
33. Crowl JT, Gray EE, Pestal K, Volkman HE, Stetson DB (2017) Intracellular nucleic acid detection in autoimmunity. *Annu Rev Immunol* 35: 313–336
34. Choubey D, Panchanathan R (2017) Absent in Melanoma 2 proteins in SLE. *Clin Immunol* 176: 42–48
35. Sester DP, Sagulenko V, Thygesen SJ, Cridland JA, Loi YS, Cridland SO, Masters SL, Genske U, Hornung V, Andoniu CE et al (2015) Deficient NLRP3 and AIM2 inflammasome function in autoimmune NZB mice. *J Immunol* 195: 1233–1241
36. Ichii O, Kamikawa A, Otsuka S, Hashimoto Y, Sasaki N, Endoh D, Kon Y (2010) Overexpression of interferon-activated gene 202 (Ifi202) correlates with the progression of autoimmune glomerulonephritis associated with the MRL chromosome 1. *Lupus* 19: 897–905
37. Santiago-Raber ML, Baccala R, Haraldsson KM, Choubey D, Stewart TA, Kono DH, Theofilopoulos AN (2003) Type-I interferon receptor deficiency reduces lupus-like disease in NZB mice. *J Exp Med* 197: 777–788
38. Carpenter S, Ricci EP, Mercier BC, Moore MJ, Fitzgerald KA (2014) Post-transcriptional regulation of gene expression in innate immunity. *Nat Rev Immunol* 14: 361–376
39. Johnstone RW, Kershaw MH, Trapani JA (1998) Isotypic variants of the interferon-inducible transcriptional repressor IFI 16 arise through differential mRNA splicing. *Biochemistry* 37: 11924–11931
40. Ma F, Li B, Yu Y, Iyer SS, Sun M, Cheng G (2015) Positive feedback regulation of type I interferon by the interferon-stimulated gene STING. *EMBO Rep* 16: 202–212
41. Robertson G, Hirst M, Bainbridge M, Bilenky M, Zhao Y, Zeng T, Euskirchen G, Bernier B, Varhol R, Delaney A et al (2007) Genome-wide profiles of STAT1 DNA association using chromatin immunoprecipitation and massively parallel sequencing. *Nat Methods* 4: 651–657
42. Orzalli MH, DeLuca NA, Knipe DM (2012) Nuclear IFI16 induction of IRF-3 signaling during herpesviral infection and degradation of IFI16 by the viral ICPO protein. *Proc Natl Acad Sci USA* 109: E3008-17
43. Bawadekar M, De Andrea M, Gariglio M, Landolfo S (2015) Mislocalization of the interferon inducible protein IFI16 by environmental insults: implications in autoimmunity. *Cytokine Growth Factor Rev* 26: 213–219
44. Ishikawa H, Ma Z, Barber GN (2009) STING regulates intracellular DNA-mediated, type I interferon-dependent innate immunity. *Nature* 461: 788–792
45. Ablasser A, Schmid-Burgk JL, Hemmerling I, Horvath GL, Schmidt T, Latz E, Hornung V (2013) Cell intrinsic immunity spreads to bystander cells via the intercellular transfer of cGAMP. *Nature* 503: 530–534
46. Wang PH, Fung SY, Gao WW, Deng JJ, Cheng Y, Chaudhary V, Yuen KS, Ho TH, Chan CP, Zhang Y et al (2018) A novel transcript isoform of STING that sequesters cGAMP and dominantly inhibits innate nucleic acid sensing. *Nucleic Acids Res* 46: 4054–4071
47. Ni X, Ru H, Ma F, Zhao L, Shaw N, Feng Y, Ding W, Gong W, Wang Q, Ouyang S et al (2016) New insights into the structural basis of DNA recognition by HINa and HINb domains of IFI16. *J Mol Cell Biol* 8: 51–61
48. Bartok E, Bauernfeind F, Khaminets MG, Jakobs C, Monks B, Fitzgerald KA, Latz E, Hornung V (2013) iGLuc: a luciferase-based inflammasome and protease activity reporter. *Nat Methods* 10: 147–154
49. Johnson KE, Chikoti L, Chandran B (2013) Herpes simplex virus 1 infection induces activation and subsequent inhibition of the IFI16 and NLRP3 inflammasomes. *J Virol* 87: 5005–5018
50. de Almeida L, Khare S, Misharin AV, Patel R, Ratsimandresy RA, Wallin MC, Perlman H, Greaves DR, Hoffman HM, Dorfleutner A et al (2015) The PYRIN domain-only protein POP1 inhibits inflammasome assembly and ameliorates inflammatory disease. *Immunity* 43: 264–276
51. Khare S, Ratsimandresy RA, de Almeida L, Cuda CM, Rellick SL, Misharin AV, Wallin MC, Gangopadhyay A, Forte E, Gottwein E et al (2014) The PYRIN domain-only protein POP3 inhibits ALR inflammasomes and regulates responses to infection with DNA viruses. *Nat Immunol* 15: 343–353



52. Matusiak M, Van Opdenbosch N, Lamkanfi M (2015) CARD- and pyrin-only proteins regulating inflammasome activation and immunity. *Immunol Rev* 265: 217–230
53. Liu T, Tang Q, Liu K, Xie W, Liu X, Wang H, Wang RF, Cui J (2016) TRIM11 Suppresses AIM2 Inflammasome by Degrading AIM2 via p62-Dependent Selective Autophagy. *Cell Rep* 16: 1988–2002
54. Veeranki S, Duan X, Panchanathan R, Liu H, Choubey D (2011) IFI16 protein mediates the anti-inflammatory actions of the type-I interferons through suppression of activation of caspase-1 by inflammasomes. *PLoS ONE* 6: e27040
55. Nakaya Y, Lilue J, Stavrou S, Moran EA, Ross SR (2017) AIM2-Like receptors positively and negatively regulate the interferon response induced by cytosolic DNA. *MBio* 8: e00944–17
56. Jakobsen MR, Paludan SR (2014) IFI16: at the interphase between innate DNA sensing and genome regulation. *Cytokine Growth Factor Rev* 25: 649–655
57. Gariano GR, Dell'Oste V, Bronzini M, Gatti D, Luganini A, De Andrea M, Gribaudo G, Gariglio M, Landolfo S (2012) The intracellular DNA sensor IFI16 gene acts as restriction factor for human cytomegalovirus replication. *PLoS Pathog* 8: e1002498
58. Johnson KE, Bottero V, Flaherty S, Dutta S, Singh VV, Chandran B (2014) IFI16 restricts HSV-1 replication by accumulating on the hsv-1 genome, repressing HSV-1 gene expression, and directly or indirectly modulating histone modifications. *PLoS Pathog* 10: e1004503
59. Lo Cigno I, De Andrea M, Borgogna C, Albertini S, Landini MM, Peretti A, Johnson KE, Chandran B, Landolfo S, Gariglio M (2015) The nuclear DNA sensor IFI16 acts as a restriction factor for human papillomavirus replication through epigenetic modifications of the viral promoters. *J Virol* 89: 7506–7520
60. Lui PY, Wong LR, Ho TH, Au SWN, Chan CP, Kok KH, Jin DY (2017) PACT facilitates RNA-induced activation of MDA5 by promoting MDA5 oligomerization. *J Immunol* 199: 1846–1855
61. Kok KH, Lui PY, Ng MH, Siu KL, Au SW, Jin DY (2011) The double-stranded RNA-binding protein PACT functions as a cellular activator of RIG-I to facilitate innate antiviral response. *Cell Host Microbe* 9: 299–309
62. Abe T, Harashima A, Xia T, Konno H, Konno K, Morales A, Ahn J, Gutman D, Barber GN (2013) STING recognition of cytoplasmic DNA instigates cellular defense. *Mol Cell* 50: 5–15
63. Zhang Y, Yang J, Zhang J, Sun L, Hirankarn N, Pan HF, Lau CS, Chan TM, Lee TL, Leung AM et al (2016) Genome-wide search followed by replication reveals genetic interaction of CD80 and ALOX5AP associated with systemic lupus erythematosus in Asian populations. *Ann Rheum Dis* 75: 891–898
64. Kew C, Lui PY, Chan CP, Liu X, Au SW, Mohr I, Jin DY, Kok KH (2013) Suppression of PACT-induced type I interferon production by herpes simplex virus 1 Us11 protein. *J Virol* 87: 13141–13149